

# Transport of Cu(II) from an Albumin Mimic Peptide, GlyGlyHisGly, to Histidine and Penicillamin.

メタデータ	言語: eng 出版者: 公開日: 2017-10-04 キーワード (Ja): キーワード (En): 作成者: メールアドレス: 所属:
URL	<a href="http://hdl.handle.net/2297/11529">http://hdl.handle.net/2297/11529</a>

**Transport of Cu(II) from an Albumin Mimic Peptide, GlyGlyHisGly,  
to Histidine and Penicillamine.**

**Akira Hanaki<sup>a\*</sup> and Akira Odani<sup>b\*</sup>**

<sup>a</sup> National Institute of Radiological Sciences,  
Anagawa 4-9-1, Inage-Ku, Chiba 263-8555, Japan

<sup>b</sup> Department of Chemistry, Graduate School of Science, Nagoya University,  
Furo-Cho, Chikusa-Ku, Nagoya 464-8602, Japan

\* Corresponding authors :

Akira HANAKI

TEL / FAX : +81-47-466-5970

Akira ODANI

TEL / FAX : +81-52-789-2954

E-mail : b42170a@nucc.cc.nagoya-u.ac.jp

## Abstract

Cu in blood has been believed to transport into cell via albumin and some amino acids. To shed light the Cu transport process we studied the reaction of the Cu(II)-peptide with the amino acid by absorption and CD spectra. Albumin mimic peptides GlyGly-L-HisGly (GGHG) and penta-Gly(G5) formed stable 4N coordinated Cu(II) complexes, but in the reaction with histidine (His) and penicillamine (Pes) the ternary Cu(II) complex formations were observed different by the kinetic study. Cu(II)-G5 complexes reacted with Pes to form the ternary complex  $\text{Cu}(\text{H}_{-1}\text{G5})(\text{Pes}^-)$  which was subsequently transformed to the binary complex  $\text{Cu}(\text{Pes}^-)_2$ . In the system with GGHG the Cu(II) was also transported from GGHG to Pes, but the ternary  $\text{Cu}(\text{H}_{-1}\text{GGHG})(\text{Pes}^-)$  complex as the intermediate was detected a trace. The ternary complex would be spontaneously transformed to  $\text{Cu}(\text{Pes}^-)_2$  upon forming, because the rate constant of the ternary complex formation  $k_{1+} = \sim 2 \text{ M}^{-1} \text{ s}^{-1}$  was less than  $k_{2+} = \sim 5 \times 10^2 \text{ M}^{-2} \text{ s}^{-1}$  for the  $\text{Cu}(\text{Pes}^-)_2$  formation at physiological pH. In the Cu(II)-GGHG – His system the ternary  $\text{Cu}(\text{H}_{-1}\text{GGHG})(\text{His})$  complex was also hardly identified because the formation constant  $K_1$  and  $k_{1+}$  were very small and the equilibrium existed between  $\text{Cu}(\text{H}_{-2}\text{GGHG})$  and  $\text{Cu}(\text{His})_2$  and its overall equilibrium constant  $\beta_2$  for  $\text{Cu}(\text{His})_2$  was very small to be  $1.00 \pm 0.05 \text{ M}^{-1}$  at pH 9.0. These results indicated that the ternary complex is formed in the Cu transport process from the albumin to the amino acid, but His imidazole nitrogen in the fourth-binding site of Cu(II) strongly resists the replacement by the incoming ligand.

Keywords; Cu(II) transport; ternary complex; GlyGly-L-HisGly; GlyGlyGlyGlyGly; histidine; penicillamine; kinetic study

## 1. Introduction

Albumin was first identified as the plasma protein most likely to bind ionic copper [1]. After administration of the isotopic copper ion to rats, or upon mixing it directly with rat plasma, albumin was labeled with  $^{67}\text{Cu}$  [2,3]. After ionic copper is transferred across the membrane of intestines, it appears in portal serum attached to albumin, histidine (His), or both [4]. The transporter recognized Cu as  $\text{Cu}(\text{His})_2$  complex, although Cu and His were taken up separately by distinct pathways [5]. This led to the hypothesis that Cu is transferred from albumin as the initial carrier to His and then to the transporter in the cell [6]. There was another suggestion, however, that Cu is probably bound to albumin *via* a  $\text{Cu}(\text{albumin})(\text{His})$  ternary complex [4].

A high affinity binding site of albumin was identified to be N-terminal three amino-acid residues [7-10], which are Asp-Ala-His for human serum albumin (HSA), and Asp-Thr-His for bovine serum albumin (BSA). In the albumin from dog and swine, the His residue at the third position is replaced by Tyr [11-13]. The replacement of His by Tyr resulted in a low affinity of Cu(II) by the model peptide study. It has been a consensus that the Cu(II)-binding site of many mammalian albumin involves the N-terminal amino nitrogen, two intervening deprotonated amide-nitrogens, and the imidazole nitrogen of the histidine residue at the third position.

The chemical interest in the Cu(II) transport in the blood has been focused on whether the ternary  $\text{Cu}(\text{albumin})(\text{His})$  complex is involved or not [14]. The ternary complex is considered to be important as the intermediate of Cu transport from outside into the cell. In order to get the information about the involvement of the  $\text{Cu}(\text{albumin})(\text{His})$  in the transport process, the peptides GlyGlyHis-X have been used as a mimic of serum albumin. The solution equilibrium studies on the Cu(II) complex formation with GlyGly-L-His and His were repeatedly studied [15,16]. It was reported that  $\text{Cu}(\text{H}_{-1}\text{GlyGly-L-His}$  and  $\text{H}_{-2}\text{GlyGly-L-His})(\text{His})$  were major species [15]. On the other hand, there was the opposite report that major species in the equilibrium state were  $\text{Cu}(\text{H}_{-2}\text{GlyGly-L-His})$  and  $\text{Cu}(\text{L-His})_2$  but not the ternary complexes [16]. Thus, the involvement of

the ternary complexes in the copper transport remained inconclusive in spite of exhaustive studies in aqueous solution.

Cu(II) outside the cell has been believed to encounter the reducing molecule involving with SH group to reduce Cu(I). To obtain the detailed mechanism we have been investigating the dynamics and statics of the reaction between Cu(II)-glycine peptide complex,  $\text{Cu}(\text{H}_{-i}\text{L})$  ( $i = 1, 2, \text{ or } 3$ ) and Cysteine (Cys), where L denotes the anionic peptide and  $-i$  means a  $i$ -th deprotonation of the amide moiety due to the Cu-N bond formation [17]. In addition aminothiols (Rs) such as Cys and penicillamine (Pes) were useful for proving the existence of short-lived intermediate Cu(II) complexes such as  $\text{Cu}(\text{H}_{-1}\text{L})(\text{Rs}^-)$  and  $\text{Cu}(\text{Rs}^-)_2$ , because these intermediates exhibited the intense  $\text{S}^- \rightarrow \text{Cu}(\text{II})$  charge transfer (LMCT) absorptions in the UV region. The presence of the ternary complex was also observed in His containing tripeptide systems except GlyGly-L-His. In the reaction with GlyGly-L-His the detectable species was limited to  $\text{Cu}(\text{Cys}^-)_2$  [18].

In order to shed light on the Cu transport from a chemical view-point, we investigated thoroughly the Cu(II) transport process by using GlyGly-L-HisGly (GGHG) and penta-Gly (G5) as albumin model, and Pes and His as 2-nd Cu carrier. The Cu(II)-G5 complex involves four species, including  $\text{CuL}$ ,  $\text{Cu}(\text{H}_{-1}\text{L})$ ,  $\text{Cu}(\text{H}_{-2}\text{L})$ , and  $\text{Cu}(\text{H}_{-3}\text{L})$  as shown  $pK_{c1}$  6.00,  $pK_{c2}$  7.81, and  $pK_{c3}$  7.89 [19], and  $\text{Cu}(\text{H}_{-3}\text{L})$  is a stable species with a 4N-coordination (Fig. 1). G5 is considered to be better than terta-Gly because of its high stability constant of  $\text{Cu}(\text{H}_{-3}\text{L})$ . GGHG can also form the stable Cu(II) complex  $\text{Cu}(\text{H}_2\text{GGHG})$  with a 4N-coordination (Fig. 1). The difference in coordination modes for those two complexes is the fourth binding-site of the Cu(II). The fourth donor in  $\text{Cu}(\text{H}_{-3}\text{G5})$  is the deprotonated amide nitrogen of the third peptide bond, while the fourth-donor in  $\text{Cu}(\text{H}_{-2}\text{GGHG})$  is the imidazole nitrogen of His. The transport of Cu(II) in  $\text{Cu}(\text{H}_{-i}\text{L})$  is triggered off by the ligand replacement in the fourth-binding site [17], so that the

nature of the fourth-donor in  $\text{Cu}(\text{H}_1\text{L})$  is important in deciding the easiness of the ternary complex formation.

The ternary complex involving  $\text{Cu}(\text{II})\text{-S}^-$  bond can be characterized by its LMCT absorption. Pes and Cys showed similar LMCT, however, Pes is good for pursuing the intermediate because of its low reaction rate. The  $\text{Cu}(\text{II})\text{-N}(\text{His})$  bond could be identified by its proper CD spectrum, however, the CD spectrometry has not been suitable for the kinetic study because of its low response and sensitivity. Here, the formation of  $\text{Cu}(\text{H}_1\text{GGHG})(\text{His})$  was discussed on the basis of the results from not only the static study of the complex formation with His and N-acetyl-histidine (AHis) but also the kinetic study of the Pes reaction. In addition, the results from the reaction of  $\text{Cu}(\text{H}_3\text{G5})$  with Pes was referred, in order to elucidate the nature for the formation of ternary complexes involving  $\text{Cu}(\text{H}_1\text{GGHG})(\text{Pes}^-)$  and  $\text{Cu}(\text{H}_1\text{GGHG})(\text{His})$ .

## 2. Experimental

### 2.1. Materials

GGHG and G5 were products from BACHEM Feinchemikalien AG.(Switzerland). They were pure, as checked by liquid chromatography. Copper(II) perchlorate,  $\text{Cu}(\text{ClO}_4)_2 \cdot 6\text{H}_2\text{O}$  from G. Frederick Smith Chem. Co.(Columbus, Oh) was used after recrystallization from hot water. Pes and His were products of Sigma Chemical Co.(St. Louis, Mo). All other chemicals were the purest of commercially available and used without further purification.

### 2.2. Preparation of sample solutions

A stock solution of Cu(II) was prepared by dissolving  $\text{Cu}(\text{ClO}_4)_2 \cdot 6\text{H}_2\text{O}$  in purified water and standardized by titration with 0.01 M EDTA with murexide as an indicator [20]. The water was deionized once and distilled from alkaline permanganate in glass apparatus, and then distilled. Solutions of the Cu(II) complexes were freshly prepared by using aliquots of the standardized Cu(II) solution with a 5 mole % excess peptide to ensure complex formation. Solutions of Pes and His were freshly prepared just prior to using. The ionic strength (I) was maintained at 0.1 M with  $\text{NaClO}_4$ .

### 2.3. Kinetics measurements of absorption spectrum in the Pes reactions with $\text{Cu}(\text{H}_i\text{GG5})$ and with $\text{Cu}(\text{H}_{-2}\text{GGHG})$

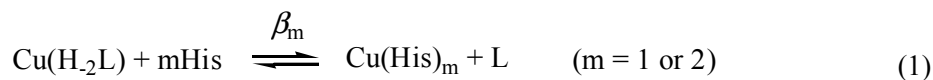
The solutions of the standardized  $1.00 \times 10^{-3}$  M  $\text{Cu}(\text{H}_i\text{GGHG})$  and five molar equivalents Pes in 0.01 M borate buffer at pH 8.5 were pre-equilibrated at 25°C under  $\text{N}_2$ . After equilibration for 20 min, the reaction started by mixing both solutions at 8 kg/cm<sup>2</sup> under  $\text{N}_2$ . The subsequent absorbance changes were recorded on a computerized Union RA-401 stopped-flow spectrophotometer equipped with a 5 mm quartz cell. The measurements were made over the range from 250 nm to 700 nm, at intervals of either 5 nm or 10 nm, and repeated at least 7 runs.

The absorption spectrum of the transient was prepared by a point-by-point method plotting the absorbance against the wavelength [17]. The species distribution relative to the reaction time was calculated by the method reported previously [17]. The dead time (DT) of the instrument determined by the reaction of ascorbate with 2,4-dichlorophenolindophenol was 1.2 ms [21]. The spectrometer was calibrated by the method reported previously [17].

The reactions were carried out under pseudo first-ordered conditions using a large excess of Pes at pH 7.5~11.0 and 25 °C ( $I = 0.1\text{M NaClO}_4$ ). A  $1.10 \times 10^{-4}$  M  $\text{Cu}(\text{H}_{-1}\text{G5})$  or  $\text{Cu}(\text{H}_{-2}\text{GGHG})$  solution was mixed with the Pes solutions and the subsequent absorbance changes at 335 nm and 385 nm were recorded on a Union RA-401 stopped-flow spectrophotometer. The pseudo-first order rate constant,  $k_{\text{obsd}}$ , was obtained by  $\ln \Delta\text{Abs}(t)$  vs time plot; where Abs was an abbreviation for absorbance and  $\Delta \text{Abs}(t) = (\text{Abs}_{\text{max}} - \text{Abs}(t))/\text{Abs}_{\text{max}}$ . Plots of  $k_{\text{obsd}}$  against [Pes] gave a straight line, and the forward rate constant ( $k_+$ ) and backward rate constant ( $k_-$ ) were obtained from the slope and the intercept on the ordinate, respectively [22,23]. The rate constants of the formations of  $\text{Cu}(\text{H}_{-1}\text{L})(\text{Pes})$  and  $\text{Cu}(\text{Pes})_2$ , expressed as  $k_{1+}$  and  $k_{2+}$ , was simultaneously obtained from the  $\ln \Delta\text{Abs}(t)$ -time curves at 335 nm and  $k_{2+}$  was obtained at 385 nm, respectively.

#### 2.4. Determination of the formation constant by CD spectrometry

The overall equilibrium constant  $\beta_m$  for the reaction of  $\text{Cu}(\text{H}_{-2}\text{GGHG})$  with L/D-His, given in Eq. (1), was determined by the molar-ratio method [24].



where the proton and the charge were omitted for simplicity. The total concentration of  $\text{Cu}(\text{H}_{-2}\text{GGHG})$   $[\text{Cu}(\text{H}_{-1}\text{L})]_0$  was arranged to be constant, and the total concentration of His  $[\text{His}]_0$  was used as the variable [21]. The equilibrium constant  $\beta_m$  is given as:

$$\beta_m = \frac{[\text{Cu}(\text{His})_m][\text{L}]}{[\text{Cu}(\text{H}_{-1}\text{L})][\text{His}]^m} = \frac{\alpha^2}{(1-\alpha)(n-m\alpha)^m [\text{Cu}(\text{H}_{-1}\text{L})]_0^{m-1}} \quad (2)$$

where the term  $\alpha$  denotes the molar fraction of the produced  $\text{Cu}(\text{His})_m$ , which can be obtained by

the ratio of ellipticity,  $\theta/\theta_{\max}$ , and  $n$  is the molar ratio  $[\text{His}]_0 / \text{the total copper } [\text{Cu}(\text{H}_{-1}\text{L})]_0$ . The measurements were carried out at 685 nm, and  $\beta_m$  was determined by the best fit at  $m = 2$  for the plot of  $(1 - \alpha)$  against  $[\alpha / (n - 2\alpha)]^2$ . The CD spectrum was recorded at 25°C on a JASCO J-20B automatic spectropolarimeter, which was standardized against a 0.12 M Ni-tartrate solution before the measurement [25].

### 3. Results

#### 3.1. Formation of the ternary complexes in the reactions of the Cu complexes with Pes

The Cu(II) transport from the peptide L to Pes was a consecutive reaction. The ternary  $\text{Cu}(\text{H}_1\text{L})(\text{Pes}^-)$  complex was produced as the intermediate and the Cu(II) was trapped as  $\text{Cu}(\text{Pes}^-)_2$  by Pes (Fig. 1). These complex species  $\text{Cu}(\text{H}_1\text{L})(\text{Pes}^-)$  and  $\text{Cu}(\text{Pes}^-)_2$  can be clearly distinguished on the absorption spectra because the former exhibited LMCT absorption at around 330 nm while the latter showed around 330 nm and 390 nm. In the reaction of  $\text{Cu}(\text{H}_{-1}\text{G5})$  and Pes the spectral data on the stopped-flow spectrometry showed the formation of  $\text{Cu}((\text{H}_{-1}\text{G5})(\text{Pes}^-))$  [17].

After mixing  $\text{Cu}(\text{H}_{-1}\text{GGHG})$  with D-Pes the transient absorption spectra for initial 100 ms at pH 8.5 were depicted in Fig. 2. Each spectrum exhibited the LMCT absorptions at 335 nm and 385 nm and these peaks were assignable to  $\text{Cu}(\text{L/D-Pes}^-)_2$  and the formation of the ternary complex  $\text{Cu}(\text{H}_{-1}\text{GGHG})(\text{Pes}^-)$  was hardly certified by the stopped-flow spectrometry. From the absorbance changes at 335 nm and 385 nm the time-dependent distributions of  $\text{Cu}(\text{H}_{-2}\text{GGHG})$ ,

$\text{Cu}(\text{H}_{-1}\text{GGHG})(\text{Pes}^-)$ , and  $\text{Cu}(\text{Pes}^-)_2$  species were estimated as following:

The observed absorbance at the time  $t$ ,  $\text{Abs}(t)$ , can be represented by

$$\text{Abs}(t) = \varepsilon^{\text{pr}}[\text{Cu}(\text{H}_2\text{L})](t) + \varepsilon^{\text{ter}}[\text{Cu}(\text{H}_1\text{L})(\text{Pes}^-)](t) + \varepsilon^{\text{bi}}[\text{Cu}(\text{Pes}^-)_2](t), \quad (3)$$

where  $\varepsilon^{\text{pr}}$ ,  $\varepsilon^{\text{ter}}$ , and  $\varepsilon^{\text{bi}}$  represent the molar absorptivity for  $\text{Cu}(\text{H}_2\text{L})$ ,  $\text{Cu}(\text{H}_1\text{L})(\text{Pes}^-)$ , and  $\text{Cu}(\text{Pes}^-)_2$ , respectively. Since  $\text{Cu}(\text{H}_2\text{L})$  exhibited no strong absorption in the UV region, Eq. (3) can be simplified as Eq. (3')

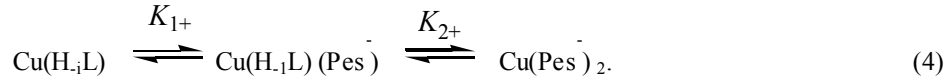
$$\text{Abs}(t) = \varepsilon^{\text{ter}}[\text{Cu}(\text{H}_1\text{L})(\text{Pes}^-)](t) + \varepsilon^{\text{bi}}[\text{Cu}(\text{Pes}^-)_2](t). \quad (3')$$

As the  $\varepsilon^{\text{ter}}$  and  $\varepsilon^{\text{bi}}$  are experimentally obtainable,  $\text{Abs}(t)$  could be resolved into  $\text{Abs}(t)^{\text{ter}}$  and  $\text{Abs}(t)^{\text{bi}}$  at each wavelength. A detailed procedure for the calculation was previously reported [17].

The time-dependent distribution of  $\text{Cu}(\text{H}_{-2}\text{GGHG})$ ,  $\text{Cu}(\text{H}_{-1}\text{GGHG})(\text{Pes}^-)$ , and  $\text{Cu}(\text{Pes}^-)_2$  for initial 200 s was shown in Fig. 3, visualizing that trace  $\text{Cu}(\text{H}_{-1}\text{GGHG})(\text{Pes}^-)$  was formed at initial 60 s. The maximum amount of  $\text{Cu}(\text{H}_{-1}\text{GGHG})(\text{Pes}^-)$  observed at 4 s was estimated to be approximately 2.5% of the total copper.  $\text{Cu}(\text{Pes}^-)_2$  reached at 150 s to a maximum, ca 75% of the total copper and the residual 25% included  $\text{Cu}(\text{H}_{-2}\text{GGHG})$  and trace  $\text{Cu}(\text{I})$  species. Those results suggested that the  $\text{Cu}(\text{II})$  in  $\text{Cu}(\text{H}_{-2}\text{GGHG})$  was likely to be transformed to  $\text{Pes}$  without forming the ternary  $\text{Cu}(\text{H}_{-1}\text{GGHG})(\text{Pes}^-)$  species.

### 3.2. Kinetics study of the reaction with *Pes* species

The  $\text{Cu}(\text{II})$  in  $\text{Cu}(\text{H}_1\text{L})$  is transported to the  $\text{Pes}$  through  $\text{Cu}(\text{H}_1\text{L})(\text{Pes}^-)$  as following:



The  $K_1$  and  $K_2$  values were obtained as the ratio of  $(k_{1+}/k_{1-})$  and  $(k_{2+}/k_{2-})$ , respectively. The rate constants  $k_{1+}$  and  $k_{2+}$  and equilibrium constants  $\log K_1$  and  $\log K_2$  in Eq. (4) were shown in Table 1.

These rate and equilibrium constants depended on pH since the concentration of the chemical species in solution are dependent on pH.

The rate of the forward-reaction,  $v$ , for the  $\text{Cu(H}_{-2}\text{L)}(\text{Pes}^-)$  formation is given by Eq (5):

$$v = k_{1+} [\text{Cu(H}_{-1}\text{L)}][\text{Pes}], \quad (5)$$

where  $[\text{Cu(H}_{-1}\text{L)}]$  and  $[\text{Pes}]$  represent the concentrations of  $\text{Cu(H}_{-1}\text{L)}$  and  $\text{Pes}$ , respectively.

Under the conditions examined, from pH 7 to pH 11, both  $\text{Cu(H}_{-1}\text{L)}$  and  $\text{Pes}$  involve several ionized species with various reactivities.  $\text{Cu(H}_{-1}\text{L)}$  involves three species [19], and  $\text{Pes}$  involves three species,  $\text{PesH}$ ,  $\text{Pes}^\pm$ , and  $\text{Pes}^-$ , which are equilibrate with the  $pK_{a2}$  7.9 and  $pK_{a3}$  10.7 [27-29]. Since the distribution of those six species depended on pH, as shown in Fig. 4, Eq. (5) can be rearranged as:

$$v = \mathbf{A}[\text{Cu(H}_{-1}\text{L)}]_0 \mathbf{B} [\text{Pes}]_0 \quad (6)$$

$[\text{Cu(H}_{-1}\text{L)}]_0$  and  $[\text{Pes}]_0$  represent the total concentrations of  $\text{Cu(H}_{-1}\text{L)}$  and  $\text{Pes}$ , respectively, and can

be written as:

$$[\text{Cu(H}_{-1}\text{L)}]_0 = [\text{Cu(H}_{-1}\text{L)}] + [\text{Cu(H}_{-2}\text{L)}] + [\text{Cu(H}_{-3}\text{L)}] \quad (7)$$

$$[\text{Pes}]_0 = [\text{PesH}] + [\text{Pes}^\pm] + [\text{Pes}^-] \quad (8)$$

**A** and **B** are given by Eqs. (9) and (10):

$$\mathbf{A} = \frac{(k_{\text{Cu(H-1L)}}[\text{H}^+]^2 + k_{\text{Cu(H-2L)}}K_{\text{c2}}[\text{H}^+] + k_{\text{Cu(H-3L)}}K_{\text{c2}}K_{\text{c3}})}{([\text{H}^+]^2 + K_{\text{c2}}[\text{H}^+] + K_{\text{c2}}K_{\text{c3}})} \quad (9)$$

where  $k_{\text{Cu(H-1L)}}$ ,  $k_{\text{Cu(H-2L)}}$ , and  $k_{\text{Cu(H-3L)}}$  are the rate constants of the  $\text{Cu(H}_{-1}\text{L})(\text{Pes}^-)$  formation concerning  $\text{Cu(H}_{-1}\text{L)}$ ,  $\text{Cu(H}_{-2}\text{L)}$ , and  $\text{Cu(H}_{-3}\text{L)}$ , respectively.

$$\mathbf{B} = \frac{(k_{\text{PesH}}[\text{H}^+]^2 + k_{\text{Pes}^\pm}K_{\text{c2}}[\text{H}^+] + k_{\text{Pes}^-}K_{\text{c2}}K_{\text{c3}})}{([\text{H}^+]^2 + K_{\text{a2}}[\text{H}^+] + K_{\text{a2}}K_{\text{a3}})} \quad (10)$$

where  $k_{\text{PesH}}$ ,  $k_{\text{Pes}^\pm}$ , and  $k_{\text{Pes}^-}$  represent the rate constants of the  $\text{Cu(H}_{-1}\text{L})(\text{Pes}^-)$  formation concerning the corresponding Pes species.

In the reaction of  $\text{Cu(H}_{-1}\text{G5)}$  with Pes the pH profiles of  $k_{1+}$  in Fig. 5 appears to consist of three phases. Between pH 8.0 and pH 9.0 both the rate constant  $k_{1+}$  and the stability constant  $K_1$  did not change significantly. Below pH 8.0 the  $k_{1+}$  increased again and at pH 7 the rate was unmeasurably rapid; the second-order rate constant determined by the stopped-flow spectrophotometer to be  $1 \times 10^7 \text{ M}^{-1} \text{ s}^{-1}$ . This is due to the increment of highly reactive  $\text{Cu(H}_{-1}\text{G5)}$  species with  $\text{N}_2\text{O}_2$  coordination since  $\text{Cu(H}_{-1}\text{GlyGly)}$  with  $\text{N}_2\text{O}_2$  coordination was shown to react at unmeasurably rapid speed [26]. The  $k_{1+}$  and  $K_1$  increased with the pH increment above pH 9.0 since the concentrations of reactive  $\text{Pes}^-$  increased depending on the pH increment.

The pH- $k_{1+}$  plots for  $\text{Cu(H}_{-1}\text{G5)}$ -Pes system was shown in Fig. 5. Referring to the distribution curves in Fig. 4, the  $\text{Cu(H}_{-3}\text{L)}$  species existed more than 50% of the total  $\text{Cu(II)}$  above pH 8 can encounter with Pes species involving with  $\text{PesH}$ ,  $\text{Pes}^\pm$ , and  $\text{Pes}^-$ . The pH- $k_{1+}$  plot above pH 8 could be elucidated by Eq. (11-1):

$$k_{1+(CuH_3L)(Pes)} = k_{1+(CuH_3L)(PesH)} + k_{1+(CuH_3L)(Pes^\pm)} + k_{1+(CuH_3L)(Pes^-)} \quad (11-1)$$

In the pH region from 7 to 8, the  $Cu(H_{-2}L)$  species is a major species and reacts with  $PesH$  and  $Pes^\pm$ , so that  $k_{1+(CuH_2L)(Pes)}$  is given by Eq. (11-2) as:

$$k_{1+(CuH_2L)(Pes)} = k_{1+(CuH_2L)(PesH)} + k_{1+(CuH_2L)(Pes^\pm)} \quad (11-2)$$

the minor  $Cu(H_{-1}L)$  species contributes to the reaction below pH 8 because the  $Cu(H_{-1}L)$  complex with a  $(N,N^-,O^-)$  or  $(N,N^-,O)$  coordination is labile toward ligand-exchange and likely to react rapidly with  $PesH$  through the proton-assisted mechanism. At neutral pH region the  $pH-k_{1+}$  plot could be elucidated by Eq. (11-3):

$$k_{1+(CuH_1L)(Pes)} = k_{1+(CuH_1L)(PeH)} + k_{1+(CuH_1L)(Pes^\pm)} \quad (11-3)$$

By combining Eqs. (11-1), (11-2), and (11-3), the full line obtained in Fig. 5 explained well the observed value.

In the reaction of  $Cu(H_{-2}GGHG)$  with  $Pes$  the  $k_{2+}$  value could not be obtained because the formation of the ternary complex was relatively slow and the rate-determining. The obtained rate constant  $k_{1+}$  values were small and increased monotonously with the pH increment as shown in Table 1 and Fig. 6. As the His imidazole N occupying the fourth-site of the  $Cu(H_{-2}GGHG)$  complex resisted the ligand-replacement by the  $PesS^-$ , the replacement reaction should occur through the nucleophilic mechanism so that the  $k_{1+}$  increased proportionally to the pH increment.

Since the  $Cu(H_{-2}GGHG)$  species is very stable and major  $Cu(II)$  species under the condition examined, Eq. (6) can be simplified as:

$$v = k_{Cu(H_{-2}L)} \mathbf{B}[Cu(H_{-2}L)]_o [Pes]_o \quad (12)$$

the  $pH-k_{1+}$  plot could be elucidated by Eq.(13):

$$k_{1+(CuH_2L)(Pes)} = k_{1+(CuH_2L)(PesH)} + k_{1+(CuH_2L)(Pes^\pm)} + k_{1+(CuH_2L)(Pes^-)} \quad (13)$$

The constants  $k_{Cu(H_1L)(PesH)}$  were expressed by the product of  $k_{Cu(H_1L)}$  and  $k(PesH)$ ; for example,  $k_{Cu(H_1L)(PesH)} = k_{Cu(H_1L)}k(PesH)$ ,  $k_{Cu(H_1L)(Pes^\pm)} = k_{Cu(H_1L)}k(Pes^\pm)$  and  $k_{Cu(H_1L)(Pes^-)} = k_{Cu(H_1L)}k(Pes^-)$ . Thus, the individual rate constants obtained from the best fits in the pH- $k_{1+}$  plots were summarized in Table 2.

### 3.3. CD study of $Cu(H_2GGHG)$ with His derivatives

The static measurement for the equilibrium between  $Cu(H_2GGHG)$  and His was carried out by using the CD spectrometric method. CD spectra measured upon mixing 0~40 equivalents L/D-His with the  $Cu(H_2GlyGly-L-HisGly)$  were shown in Fig. 7. The CD spectrum for  $Cu(H_2GGHG)$  exhibited  $\lambda_{max}$  at 500 nm ( $\Delta\epsilon = +0.984$ ) and 588 nm ( $\Delta\epsilon = -0.194$ ), while  $Cu(L-His)_2$  exhibited  $\lambda_{max}$  at 560 nm ( $\Delta\epsilon = -0.022$ ) and 685 nm ( $\Delta\epsilon = +0.453$ ) and  $Cu(D-His)_2$  did at 565 nm ( $\Delta\epsilon = 0.019$ ) and 685 nm ( $\Delta\epsilon = -0.454$ ). The CD spectra of those Cu(II) complexes could be distinguished each other. A family of the spectra showed isosbestic points at 560 nm for the  $Cu(H_2GGHG)/L-His$  system and at 560 nm and 615 nm for the  $Cu(H_2GGHG)/D-His$  system, suggesting the equilibrium between  $Cu(H_2GGHG)$  and  $Cu(His)_2$  complexes. The spectra 2~7 in Fig 7 were elucidated as the composition of two components  $Cu(H_2GGHG)$  and  $Cu(His)_2$ . The involvement of any other species such as the ternary  $Cu(H_1GGHG)(His)$  complex did not be indicated. Then,  $Cu(H_2GGHG)$  was considered to equilibrate with His as:

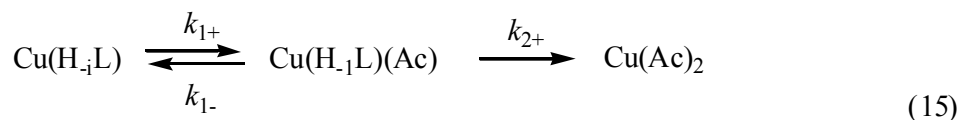


where the proton was omitted for simplicity. The value of  $m$  and the overall equilibrium constant  $\beta_m$  in Eq. (14) was determined by using Eq. (2). The best fit was obtained at  $m = 2$  and the  $\beta_2$  value in GGHG/L-His system obtained from the slope of a straight in Fig. 8 was  $\beta_2 = 1.15 \pm 0.05 \text{ M}^{-2}$  at pH 9.0. Since the GGHG/D-His systems gave similar  $\beta_2$  value as the GGHG/L-His system, the replacement reaction is no stereoselective and this supports no presence of the ternary species in the reaction mixture.

## 4. Discussion

### 4.1. Kinetics of the ternary complex formation with Pes

The Cu(II) bound to peptides has shown to be transported to the acceptor molecules (Ac) such as Pes and His through the consecutive ligand-replacement reaction (15):



If the reaction is written in a simplified equation, it may be given as  $\text{Cu(H}_i\text{L)} \rightarrow \text{Cu(H}_{i-1}\text{L)(Ac)} \rightarrow \text{Cu(Ac)}_2$  and the concentrations of the intermediate  $\text{Cu(H}_{i-1}\text{L)(Ac)}$  and product  $\text{Cu(Ac)}_2$  can be given as follows:

$$[\text{Cu(H}_{i-1}\text{L)(Ac)}] = [\text{Cu(H}_i\text{L)}]_0 \left( \frac{k_{1+}}{k_{1+} - k_{2+}} \right) (\exp(-k_{2+}t) - \exp(-k_{1+}t)) \quad (16)$$

$$[\text{Cu(Ac)}_2] = [\text{Cu(H}_i\text{L)}]_0 + [\text{Cu(H}_i\text{L)}]_0 \left\{ \frac{k_{2+}}{k_{1+} - k_{2+}} \exp(-k_{1+}t) - \left( \frac{k_{1+}}{k_{1+} - k_{2+}} \right) \exp(-k_{2+}t) \right\} \quad (17),$$

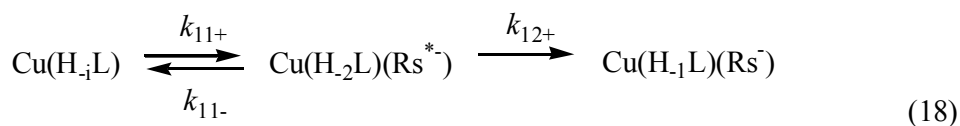
where  $k_{1+}$  and  $k_{2+}$  represent the rate constants for the  $\text{Cu(H}_{i-1}\text{L)(Ac)}$  and  $\text{Cu(Ac)}_2$  formations, respectively. The concentration of  $\text{Cu(H}_{i-1}\text{L)(Ac)}$  during the transport process is determined by the

ratio of  $k_{1+}/k_{2+}$ . In the case of  $k_{1+} > k_{2+}$ , the rate plot is resolved into two straight lines given as  $\Delta\text{Abs}(t) = \Delta\text{Abs}_1(0)\exp(-k_{1+}t) + \Delta\text{Abs}_2(0)\exp(-k_{2+}t)$ , where  $\Delta\text{Abs}(0)$  denotes  $\Delta\text{Abs}$  at  $t = 0$ . On the other hand, at  $k_{1+} < k_{2+}$ , the rate plot gives a straight line as  $\Delta\text{Abs}(t) = \Delta\text{Abs}(0)\exp(-k_{1+}t)$ . When  $k_{1+}$  is smaller than  $k_{2+}$  by one order of magnitude ( $k_{1+}/k_{2+} = 0.1$ ), the maximum amount of  $\text{Cu}(\text{H}_1\text{L})(\text{Ac})$  during the reaction was evaluated to be approximately 8 % of  $[\text{Cu}(\text{H}_1\text{L})]_0$ . At  $k_{1+}/k_{2+} = 0.01$ ,  $\text{Cu}(\text{H}_1\text{L})(\text{Ac})$  was approximately 1 % of total Cu. The reaction of  $\text{Cu}(\text{H}_2\text{GGHG})$  with Pes afforded a trace of the ternary  $\text{Cu}(\text{H}_1\text{GGHG})(\text{Pes})^-$  complex as shown in Fig. 3. From the maximum amount approximately 3 % of the  $\text{Cu}(\text{H}_1\text{GGHG})(\text{Pes})^-$  at pH 8.5 the ratio of  $k_{1+}/k_{2+}$  was evaluated to be 0.03 ~ 0.05.

The  $k_{2+}$  values for the reaction of  $\text{Cu}(\text{H}_2\text{L})$  with Rs depended on the coordination mode of the Cu(II) and the steric environments around the Cu(II) [30]. Since the  $\text{Cu}(\text{H}_1\text{GGHG})(\text{Pes})^-$  and the  $\text{Cu}(\text{H}_1\text{G5})(\text{Pes})^-$  are same 3NS coordination and similar environment around Cu(II), the  $k_{2+}$  values for both complexes are expected to be similar. As shown in Table 1, in the pH region 7.5~8.5 the  $k_{2+}$  values for the  $\text{Cu}(\text{H}_i\text{G5})(\text{Pes})^-$  ( $i = 2$  or  $3$ ) were  $36 \sim 110 \text{ M}^{-1} \text{ s}^{-1}$  and the  $k_{1+}$  for the  $\text{Cu}(\text{H}_2\text{GGHG})$  were  $2 \sim 4 \text{ M}^{-1} \text{ s}^{-1}$ , accordingly, the ratio of the  $k_{1+}/k_{2+}$  value estimated for  $\text{Cu}(\text{H}_1\text{GGHG})(\text{Pes})^-$  is 0.03-0.05. This value is same as the value 0.03 ~ 0.05 obtained from Fig. 3. This leads to the conclusion that the ternary complex  $\text{Cu}(\text{H}_1\text{GGHG})(\text{Pes})^-$  was produced during the reaction, but it presents a small portion of the total Cu(II) because the  $\text{Cu}(\text{H}_1\text{GGHG})(\text{Pes})^-$  formed is likely to undergo spontaneous reaction to  $\text{Cu}(\text{Pes})_2$  at physiological pH.

#### 4.2. Kinetic and thermodynamic factors determining the easiness of the Cu(II) transport

The replacement of the fourth-donor in  $\text{Cu}(\text{H}_{-1}\text{L})$  triggers off the  $\text{Cu}(\text{II})$  transport. In the reaction of  $\text{Cu}(\text{H}_{-1}\text{L})$  with  $\text{Rs}$ , the  $\text{Cu}(\text{H}_{-2}\text{L})(\text{Rs}^*)$  initially formed is subsequently rearranged to yield the  $\text{Cu}(\text{H}_{-1}\text{L})(\text{Rs}^-)$  [30,31]. Since the backward-reaction from the  $\text{Cu}(\text{H}_{-1}\text{L})(\text{Rs}^-)$  to the  $\text{Cu}(\text{H}_{-2}\text{L})(\text{Rs}^*)$  was far slow, the reaction can be briefly given as Eq. (18):



where  $\text{Rs}^*$  denotes the S-monodentate  $\text{Rs}^-$ . Then, the overall rate  $v$  in Eq. (5) is rewritten in Eqs. (19), (20) [30]:

$$v = k_{1+} [\text{Cu}(\text{H}_{-1}\text{L})][\text{Pes}] = k_{12+} [\text{Cu}(\text{H}_{-2}\text{L})(\text{Rs}^*)] \quad (19)$$

$$k_{1+} = k_{12+} k_{11+} / (k_{12+} + k_{11-}) = k_{12+} K_{11} / [1 + (k_{12+} / k_{11-})] \quad (20)$$

The overall rate constant  $k_{1+}$  from the  $\text{Cu}(\text{H}_{-1}\text{L})$  to the  $\text{Cu}(\text{H}_{-1}\text{L})(\text{Rs}^-)$  is the function of the formation constant  $K_{11}$  for  $\text{Cu}(\text{H}_{-2}\text{L})(\text{Rs}^*)$  and the rate constant  $k_{12+}$  for the  $\text{Cu}(\text{H}_{-1}\text{L})(\text{Rs}^-)$ . The  $k_{12+}$  was evaluated from the slope of the  $\Delta k_{1+} / \Delta K_{11}$  plot at the origin approximates when the  $k_{1+}$  was smaller than the  $k_{11+}$  [30]. As the  $\text{Cu}(\text{H}_{-2}\text{L})(\text{Rs}^*)$  and the  $\text{Cu}(\text{H}_{-2}\text{L})(\text{ARs}^-)$  ( $\text{ARs}^- = \text{N-acetyl-Rs}^-$ ) have the same 3N1S coordination structure, the  $K_{11}$  could be replaced by the formation constant  $K_1$  for  $\text{Cu}(\text{H}_{-2}\text{L})(\text{ARs}^-)$ . The transport of  $\text{Cu}(\text{II})$  involving with His is assumed to be in the same manner of the  $\text{Rs}$ . The intermediate initially formed is considered to be the ternary complex  $\text{Cu}(\text{H}_{-2}\text{L})(\text{His}^*)$ , which is the same coordination structure of the  $\text{Cu}(\text{H}_{-2}\text{L})(\text{AHis})$  shown in Fig. 9.

The  $k_{11+}$  and  $k_{12+}$  values in Eq. (18) depended on the pH, that is, the coordination mode of

the Cu(II)-peptide Cu(H<sub>-1</sub>L). The  $k_{11+}$  values in the system involving the Cu(H<sub>-2</sub>L) with N,N,N,O coordination were larger than those in the Cu(H<sub>-3</sub>L) with N,N,N,N coordination, and the  $k_{12+}$  for the Cu(H<sub>-2</sub>L)(Cys<sup>\*</sup>) with (N,N,N)(S<sup>-</sup>) donor set were  $\sim 10^5 \text{ M}^{-1} \text{ s}^{-1}$  [30]. The overall rate constant  $k_{1+}$  for the Cu(H<sub>-1</sub>GGHG)/Pes reaction were smaller than those of the Cu(H<sub>-3</sub>G5)/Pes reaction as shown in Table 1. These indicate that the imidazole N in the fourth-site of Cu(II) would strongly resist being replaced by the incoming donor and thereby  $k_{11+}$  and  $K_{11}$  values become small.

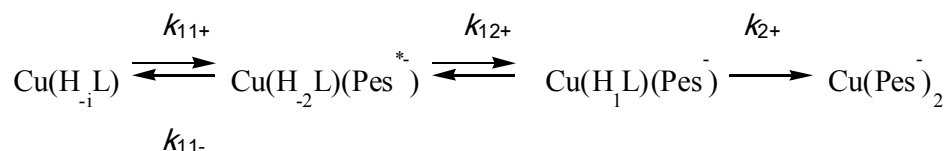
The overall rate constant  $k_{1+}$  of the Cu(H<sub>-1</sub>L)(Rs<sup>-</sup>) formation was proportional to  $K_{11}$  as well as  $k_{11+}$  [30]. The formation constants  $K_1$  for Cu(H<sub>-j</sub>L)(ACys) and Cu(H<sub>-j</sub>L)(AHis) (j = 1 or 2) for various peptide systems were shown in Table 3. The  $K_1$  values of Cu(H<sub>-j</sub>L)(AHis) were a little smaller than those of Cu(H<sub>-j</sub>L)(ACys<sup>-</sup>). Assuming that the  $k_{11+}$  values for the Cu(H<sub>-2</sub>L)(His<sup>\*</sup>) and Cu(H<sub>-2</sub>L)(Rs<sup>\*</sup>) species are similar, the  $k_{1+}$  for Cu(H<sub>-2</sub>GGHG)(His) was evaluated to be at least one order of magnitude smaller than that of Cu(H<sub>-2</sub>GGHG)(Pes<sup>-</sup>) by referring to the relative  $K_1$  values  $\Delta \log K_1$  for the Cu(H<sub>-1</sub>L)(AHis) and the Cu(H<sub>-1</sub>L)(ACys) in Table 3. At physiological pH, the  $k_{1+}$  values for the Cu(H<sub>-2</sub>G5)(Pes<sup>-</sup>) and Cu(H<sub>-2</sub>GGHG)(Pes<sup>-</sup>) formations were approximately  $1 \times 10^3 \text{ M}^{-1} \text{ s}^{-1}$  and  $2 \text{ M}^{-1} \text{ s}^{-1}$ , respectively, as shown in Table 1. Accordingly, the  $k_{11+}$  for Cu(H<sub>-2</sub>GGHG)(His<sup>\*</sup>) was estimated to be  $\sim 10^{-1} \text{ M}^{-1} \text{ s}^{-1}$  or less. Those suggest that not only the coordinated imidazole N in Cu(H<sub>-2</sub>GGHG) resists the ligand replacement reaction but also the Cu(H<sub>-2</sub>GGHG)(AHis) easily dissociates back to the Cu(H<sub>-2</sub>GGHG). The proposed reaction pathway and kinetic parameters were summarized in Fig. 10. The Cu(II) in Cu(H<sub>-2</sub>GGHG) is certainly transported to His, but considerable amounts of the ternary Cu(H<sub>-1</sub>GGHG)(His) complex is not

formed. The starting complex  $\text{Cu}(\text{H}_{-2}\text{GGHG})$  is thermodynamically stable, while the intermediate  $\text{Cu}(\text{H}_{-1}\text{GGHG})(\text{His})$  is thermodynamically unstable due to either the dissociation back to the  $\text{Cu}(\text{H}_{-2}\text{GGHG})$  or spontaneous change to  $\text{Cu}(\text{His})_2$ .

The presence of the side-chain at the N-terminal amino acid residue hindered the  $\text{Cu}(\text{II})$  transport to  $\text{Rs}^-$  since the bulky side chain made the  $k_1$  values decrease without exception. While, of much interest is that the  $k_2$  for the  $\text{Cu}(\text{H}_{-1}\text{AspGly})/\text{Cys}$  system was approximately one order magnitude bigger than the  $\text{Cu}(\text{H}_{-1}\text{GlyGly})/\text{Cys}$  system, indicating aspartic acid  $\beta$ -carboxylate group at the N terminal of HSA assists the formation of the chelate ring in the  $\text{Cu}(\text{H}_{-1}\text{L})(\text{Rs}^-)$  and stabilized the ternary intermediate complex (A. Hanaki, unpublished data). Thus, the affinity for  $\text{Cu}(\text{II})$  is important in determining the easiness of the ternary complex formation.

## 5. Conclusion .

The result of spectrometric and kinetic studies revealed that the Cu(II) bound to glycine peptide L was transported to Pes through the ternary complex  $\text{Cu}(\text{H}_{-1}\text{L})(\text{Pes}^-)$ . A series of the reactions can be briefly written as:



where  $i$  is 2 or 3, and  $\text{Pes}^*$  denotes the S-monodentate  $\text{Pes}^-$ . The overall rate constant  $k_{1+}$  from the  $\text{Cu}(\text{H}_{-1}\text{L})$  to the  $\text{Cu}(\text{H}_{-1}\text{L})(\text{Pes}^-)$  were the function of the rate constant  $k_{12+}$  and formation constant  $K_{11}$  for  $\text{Cu}(\text{H}_{-2}\text{L})(\text{Pes}^*)$  and given as  $k_{1+} = k_{12+} k_{11+} / (k_{12+} + k_{11-}) = k_{12+} K_{11} / [1 + (k_{12+} / k_{11-})]$ . In the reaction with  $\text{Cu}(\text{H}_{-2}\text{GGHG})$  involving with coordinated His imidazole a small quantity of the ternary  $\text{Cu}(\text{H}_{-1}\text{GGHG})(\text{Pes}^-)$  complex was detected because the  $k_{1+}$  was smaller than the  $k_{2+}$ .

Though the ternary  $\text{Cu}(\text{H}_{-1}\text{GGHG})(\text{Pes}^-)$  complex could formed at  $k_{1+} = \sim 2 \text{ M}^{-1} \text{ s}^{-1}$  under a physiological condition, it was immediately transformed to  $\text{Cu}(\text{Pes}^-)_2$  at 40~60-fold faster speed.

In the reaction of  $\text{Cu}(\text{H}_{-1}\text{GGHG})$  with His, the intermediate  $\text{Cu}(\text{H}_{-1}\text{GGHG})(\text{His})$  was not detected by the CD spectrometry, and  $\text{Cu}(\text{H}_{-2}\text{GGHG})$  appeared to equilibrate with  $\text{Cu}(\text{His})_2$  ( $\beta_2 = K_1 K_2 = 1.0 \text{ M}^{-2}$ ) at pH 9.0. The formation constants  $K_1$  for the  $\text{Cu}(\text{H}_{-1}\text{GGHG})(\text{His})$  may be far smaller than the  $K_2$  for  $\text{Cu}(\text{His})_2$ . On the basis of the results obtained from the  $\text{Cu}(\text{H}_{-1}\text{GGHG})/\text{Pes}$  reaction, the rate constants  $k_{1+}$  for the  $\text{Cu}(\text{H}_{-1}\text{GGHG})(\text{His})$  formation was expected to be far smaller and estimated as  $\sim 10^{-1} \text{ M}^{-1} \text{ s}^{-1}$ . The  $\text{Cu}(\text{H}_{-1}\text{GGHG})(\text{His})$ , upon forming, is immediately transformed to  $\text{Cu}(\text{His})_2$ . It is concluded that  $\text{Cu}(\text{H}_{-1}\text{GGHG})$ , the Cu(II) complex of HAS and BSA mimic

peptide, is thermodynamically stable as it approaches to His or metal-ion carriers, but the Cu(II) in  $\text{Cu}(\text{H}_{-1}\text{GGHG})(\text{His})$  is labile to allow fast exchange to be transport to its proper receptor.

## 6. Abbreviations

GGHG	GlyGly-L-HisGly
G5	penta-Gly
L	peptide (anionic form involving $\text{NH}_2$ and $\text{COO}^-$ )
BSA	bovine serum albumin
HSA	human serum albumin
LMCT	ligand to metal charge transfer
Rs	aminothiol
Cys <sup>-</sup>	L-cysteinate; $\text{SCH}_2\text{CH}(\text{NH}_2)\text{COO}^-$
Pes	penicillamine including PesH, Pes <sup>±</sup> , and Pes <sup>-</sup> (usually D form)
PesH	$\text{HSC}(\text{CH}_3)_2\text{CH}(\text{NH}_3^+)\text{COO}^-$
Pes <sup>±</sup>	$\text{SC}(\text{CH}_3)_2\text{CH}(\text{NH}_3^+)\text{COO}^-$ and $\text{HSC}(\text{CH}_3)_2\text{CH}(\text{NH}_2)\text{COO}^-$
Pes <sup>-</sup>	$\text{SC}(\text{CH}_3)_2\text{CH}(\text{NH}_2)\text{COO}^-$
ARs	N-acetyl Rs
AHis	N-acetyl-L-histidine
ACys	N-acetyl-L-cysteine
$\gamma$ -Aba	$\gamma$ -aminobutyrate
$\delta$ -Ava	$\delta$ -aminovalerate
$\text{Cu}(\text{H}_{-i}\text{L})$	the Cu(II) complex of peptide HL in which the first, second, and i-th amide groups are deprotonated
$\text{Cu}(\text{H}_j\text{L})(\text{ACys}^-)$	the ternary complexes involving with ACys <sup>-</sup> (j = 1 and 2).
Ac	acceptor molecule

## **Acknowledgments**

This work was supported in part by the Grant-in-Aid for Scientific Research (A. O.) from the Ministry of Education, Culture, Sports, Science and Technology of Japan, and the Hungary-Japan Cooperative Research Program (A. O.) from the Japan Society for Promotion of Science (JSPS), for which AO express thanks.

## References

- [1] A. G. Bearn, H. G. Kunkel, *Proc. Exptl. Biol. Med.* 85 (1954) 44-48.
- [2] K. C. Weiss, M. C. Linder, *Am. J. Physiol.* 249 (1985) E77-E88.
- [3] M. C. Linder, L. Wooten, P. Cerveza, S. Cotton, R. Schlze, N. Lomeli, *Am. J. Clin. Nutr. Suppl* 67 (1998) 965s-971s.
- [4] S. Y. Lau, T. P. A. Kruck, B. Sarkar, *J. Biol. Chem.* 249 (1974) 5878-5884.
- [5] H. J. McArdle, S. M. Gross, D. M. Danks, *J. Cell Physiol.* 136 (1988) 373-378.
- [6] R. C. Schmitt, H. M. Darwish, J. C. Cheney, M. J. Ettingrt, *Am. J. Physiol.* 244 (1983) G183-191.
- [7] E. Breslow, *J. Biol. Chem.* 239 (1964) 3252-3259.
- [8] S. Lau, B. Sarkar, *J. Biol. Chem.* 246 (1971) 5938-5943.
- [9] J. Masuoka, J. Hagenauer, B. R. Van Dyke, P. Saltman, *J. Biol. Chem.* 268 (1993) 21533-21537.
- [10] M. C. Linder, N. A. Lomeli, S. Donley, F. Mehrbod, P. Cerveza, S. Cotton, L. Wooten, *Adv. Exptl. Med. and Biol.* 448 (1999) 1-16.
- [11] G. Rakhit, B. Sarkar, *J. Inorg. Biochem.* 15 (1981) 233-241.
- [12] P. F. Predki, C. Harford, P. Brar, B. Sarkar, *Biochem. J.* 287 (1992) 211-215.
- [13] M. Volko, H. Morris, M. Mazur, J. Telser, E. J. L. McInnes, P. E. Mabbs, *J. Phys. Chem. B* 103 (1999) 5591-5597.
- [14] P. Deschamps, P. P. Kulkarni, M. Gautam-Basak, B. Sarkar, *Coord. Chem. Rev.* 249 (2005) 895-909.
- [15] T. P. A. Kruck, B. Sarkar, *Inorg. Chem.* 14 (1975) 2383-2388.
- [16] T. Sakurai, A. Nakahara, *Inorg. Chem.* 19 (1980), 847-853.
- [17] A. Hanaki, M. Hiraoka, T. Abe, Y. Funahashi, A. Odani, *Bull. Chem. Soc. Jpn.* 76 (2003) 1747-1755.

- [18] A. Hanaki, N. Ikota, J. Ueda, T. Ozawa, A. Odani, *Bull. Chem. Soc., Jpn.* 76 (2003) 2143-2150
- [19] K. Varnagy, J. Szaba, I. Sovago, G. Malandrinos, D. Sanna, G. Micera, *J. Chem. Soc. Dalton Trans.* (2000) 467-472.
- [20] G. Schwarzenbach, in: *Die komplexometrische Titration*, F. Enke, Stuttgart, (1955) p. 68.
- [21] B. Tonomura, H. Nakatani, M. Ohnishi, J. Yamaguchi-Itoh, K. Hiromi, *Anal. Biochem.* 84 (1978) 370-383.
- [22] N. Yoshida and M. Fujimoto, *Chem. Lett.* (1980) 231-234.
- [23] A. Hanaki, *Chem. Lett.* (1994) 1263-1265.
- [23] A. Hanaki, J. Ueda, N. Ikota, *Bull. Chem. Soc. Jpn.* 77 (2004) 1475-1477.
- [24] T. Konno, H. Meguro, T. Murakami, M. Hatano, *Chem. Lett.* (1981) 953-956.
- [25] A. Hanaki, T. Ozawa, Y. Funahashi, A. Odani, *Bull. Chem. Soc. Jpn.* 76 (2004) 699-707.
- [27] H. Kozlowki, J. Urbanska, I. Sovago, K. Varnagy, A. Kiss, J. Spsychala, K. Cherifi, *Polyhedron* (1990) 831-837.
- [28] J. Urbanska, H. Kozlowski, B. Kurzaki, *J. Coord. Chem.* 25 (1992) 149-154.
- [29] M. S. Nair, P. T. Arasu, M. S. Pillai. C. Natarajan, *J. Chem. Soc. Dalton Trans.* (1993) 917-921.
- [30] A. Hanaki, Y. Funahashi, A. Odanii, *J. Inorg. Biochem.* 100 (2006) 305-315.
- [31] A. Hanaki, A. Nagai, N. Ikota, *Chem. Lett.* (1995) 611-612.
- [32] A. Hanaki, J. Ueda, N. Ikota, *Bull. Chem. Soc. Jpn.* 77 (2004) 1475-1477.

Table 1

Rate constants  $k_{1+}$  and equilibrium constants  $K_1$  for the reactions of  $\text{Cu}(\text{H}_{-1}\text{G5})$  and  $\text{Cu}(\text{H}_{-2}\text{GGHG})$  with Pes.

pH	$\text{Cu}(\text{H}_{-1}\text{G5})$			$\text{Cu}(\text{H}_{-2}\text{GGHG})$		$k_{1+}/k_{2+}^a$
	$k_{1+}$ /M <sup>-1</sup> s <sup>-1</sup>	$\log K_1$ /M <sup>-1</sup>	$k_{2+}$ /M <sup>-1</sup> s <sup>-1</sup>	$\log K_2$ /M <sup>-1</sup>	$k_{1+}$ /M <sup>-1</sup> s <sup>-1</sup>	
7.5	$1.08 \times 10^3$	1.97	$3.62 \times 10$	1.27	1.83	0.05
8.0	$6.02 \times 10^2$	1.87	$7.68 \times 10$	1.63	2.18	0.03
8.5	$5.70 \times 10^2$	1.86	$1.10 \times 10^2$	1.80	4.08	0.04
9.0	$6.49 \times 10^2$	1.95	$1.28 \times 10^2$	1.86	8.56	0.07
9.5	$7.69 \times 10^2$	2.01	$1.55 \times 10^2$	1.95	$2.04 \times 10$	0.13
10.0	$1.03 \times 10^3$	2.14	$2.07 \times 10^2$	2.07	$5.41 \times 10$	0.26
10.5	$1.65 \times 10^3$	2.32	$3.29 \times 10^2$	2.28	$1.06 \times 10^2$	0.32
11.0	$2.37 \times 10^3$	2.46	$4.78 \times 10^2$	2.40	$1.95 \times 10^2$	0.40

<sup>a</sup> ratio of  $k_{1+}$  for  $\text{Cu}(\text{H}_{-2}\text{GGHG})$  to  $k_{2+}$  for  $\text{Cu}(\text{H}_{-1}\text{G5})$ .

Table 2

Rate Constants  $k_{1+}$  for the reaction of Pes with  $\text{Cu}(\text{H}_{-1}\text{G5})$  and  $\text{Cu}(\text{H}_{-2}\text{GGHG})$ .

$k_{1+}^a$	$\text{Cu}(\text{H}_{-1}\text{G5})$ / $\text{M}^{-1}\text{s}^{-1}$	$\text{Cu}(\text{H}_{-2}\text{GGHG})$ / $\text{M}^{-1}\text{s}^{-1}$
$k_{1+(\text{CuH}_{-1}\text{L})(\text{RsH})}$	$8.0 \times 10^3$	
$k_{1+(\text{CuH}_{-1}\text{L})(\text{Rs}^\pm)}$	$8.5 \times 10^2$	
$k_{1+(\text{CuH}_{-2}\text{L})(\text{RsH})}$	$3.40 \times 10^2$	1.40
$k_{1+(\text{CuH}_{-2}\text{L})(\text{Rs}^\pm)}$	$7.00 \times 10^2$	2.70
$k_{1+(\text{CuH}_{-3}\text{L})(\text{RsH})}$	$2.40 \times 10^2$	$3.00 \times 10^2$
$k_{1+(\text{CuH}_{-3}\text{L})(\text{Rs}^\pm)}$	$6.20 \times 10^2$	
$k_{1+(\text{CuH}_{-3}\text{L})(\text{Rs}^-)}$	$3.30 \times 10^3$	

<sup>a</sup>  $k_{1+(\text{CuH}_{-1}\text{L})(\text{Rs}^-)}$  and  $k_{1+(\text{CuH}_{-2}\text{L})(\text{Rs}^-)}$  were not determined because  $\text{Cu}(\text{H}_{-1}\text{G5})$  and

$\text{Cu}(\text{H}_{-2}\text{GGHG})$  could not encounter with  $\text{Pes}^-$ .

Table 3

Formation constants  $K_1$  for the ternary complexes,  $\text{Cu}(\text{H}_{-i}\text{L})(\text{ACys}^-)$  and

$\text{Cu}(\text{H}_{-i}\text{L})(\text{AHis})$  ( $i = 1$  or  $2$ ) at  $25^\circ\text{C}$

Peptide	$\log K_1 / \text{M}^{-1}$		$\Delta \log K_1^{\text{d}}$
	$\text{Cu}(\text{H}_{-i}\text{L})(\text{AHis})^{\text{a}}$	$\text{Cu}(\text{H}_{-i}\text{L})(\text{ACys}^-)^{\text{b}}$	
GlyGly	3.31	4.55	-1.24
GlyGlyGly	1.77	2.45	-0.68
GlyGly- $\beta$ -Ala	0.55	1.20	-0.65
GlyGly- $\gamma$ -Aba	2.21	3.00	-0.79
GlyGly- $\delta$ -Aba	3.24	4.66	-1.42
G5	1.30 <sup>c</sup>	2.30	-1.00
Gly- $\beta$ -Ala-Gly	-0.16	-0.43	0.27

<sup>a</sup> data at pH 10.0 from [32].

<sup>b</sup> data at pH 9.3 from [30].

<sup>c</sup> estimated by 0.99 at pH 10.5 and 3.14 at pH 7.5.

<sup>d</sup>  $\Delta \log K_1 = \log K_1(\text{Cu}(\text{H}_2\text{L})(\text{AHis})) - \log K_1(\text{Cu}(\text{H}_2\text{L})(\text{ACys}^-))$

## Figure Legend

Fig. 1. Coordination structures for  $\text{Cu}(\text{H}_{-2}\text{GGHG})$ ,  $\text{Cu}(\text{H}_{-i}\text{G5})$  ( $i = 1, 2, \text{ or } 3$ ),  $\text{Cu}(\text{H}_1\text{L})(\text{Rs})^-$ , and  $\text{Cu}(\text{Rs})_2^-$ .

Fig. 2. Transient absorption spectra in the reaction of  $\text{Cu}(\text{H}_{-2}\text{GGHG})$  with Pes at pH 8.5.  $[\text{Cu}(\text{II})] = 5.07 \times 10^{-4} \text{ M}$ ,  $[\text{Pes}] = 2.47 \times 10^{-3} \text{ M}$  (4.87 equiv), pH 8.5 ( $I = 0.1 \text{ M NaClO}_4$ ). (1) 1.2 ms (DT), (2) 20 ms, (3) 40 ms, (4) 60 ms, (5) 100 ms.

Fig. 3. Distribution of Cu(II) species during the reaction of  $\text{Cu}(\text{H}_{-2}\text{GGHG})$  and Pes at pH 8.5.

Experimental conditions were same as Fig. 2. (1)  $\text{Cu}(\text{H}_{-2}\text{L})$ , (2)  $\text{Cu}(\text{H}_{-1}\text{L})(\text{Pes})^-$ , (3)  $\text{Cu}(\text{Pes})_2^-$ .

Fig. 4. Species distribution curves for. Cu-G5-H and Pes-H systems. upper;  $\text{Cu}(\text{H}_{-i}\text{G5})$ , lower; Pes.

(1)  $\text{Cu}(\text{H}_{-1}\text{L})$ , (2)  $\text{Cu}(\text{H}_{-2}\text{L})$ , (3)  $\text{Cu}(\text{H}_{-3}\text{L})$ , (4)  $\text{PesH}$ , (5)  $\text{Pes}^{\pm}$ , (6)  $\text{Pes}^-$ .  $[\text{Cu}(\text{II})] = [\text{Pes}] = 1.0 \times 10^{-3} \text{ M}$ ,  $[\text{L}]/[\text{Cu}(\text{II})] = 1.05$ .

Fig. 5. pH profile of the rate constant  $k_{1+}$  for the reaction of  $\text{Cu}(\text{H}_{-i}\text{G5})$  with Pes.

o; observed values, (1)  $k_{1+(\text{CuH}_1\text{L})(\text{Pes})}$ , (2)  $k_{1+(\text{CuH}_2\text{L})(\text{Pes})}$ , (3)  $k_{1+(\text{CuH}_3\text{L})(\text{Pes})}$ .

Fig. 6. pH profile of the rate constant  $k_{1+}$  for the reaction of  $\text{Cu}(\text{H}_{-2}\text{GGHG})$  with L/D-Pes.

o, D-Pes,  $\Delta$ , L-Pes.

Fig. 7. CD spectra observed upon mixing  $\text{Cu}(\text{H}_{-2}\text{GGHG})$  and L/D-His at pH 9.0.

A,  $\text{Cu}(\text{H}_{-2}\text{GGHG})/\text{L-His}$  system, B,  $\text{Cu}(\text{H}_{-2}\text{GGHG})/\text{D-His}$  system.

(1)  $\text{Cu}(\text{H}_{-2}\text{GGHG})$ ; (2)-(7)  $[\text{Cu}(\text{H}_{-2}\text{GGHG})] + [\text{His}]$ , (2)  $n = 2$ , (3)  $n = 4$ , (4)  $n = 6$ , (5)  $n = 10$ , (6)  $n = 20$ , (7)  $n = 40$ ; (8)  $\text{Cu}(\text{His})_2$ .  $[\text{Cu}(\text{II})] = 2.51 \times 10^{-3} \text{ M}$ ,  $n = [\text{His}]/[\text{Cu}(\text{H}_{-2}\text{GGHG})]$ .

Fig. 8. Plots of  $(1 - \alpha)$  against  $[\alpha/(n - 2\alpha)]^2$ . Experimental conditions were same as Fig. 7.

Fig. 9. Coordination structures for  $\text{Cu}(\text{H}_{-2}\text{L})(\text{ACys}^-)$  and  $\text{Cu}(\text{H}_{-2}\text{L})(\text{AHis})$ .

Fig. 10 Proposed pathway of the Cu(II) transport from GGHG to His. Kinetic parameters are estimated values at pH 8.

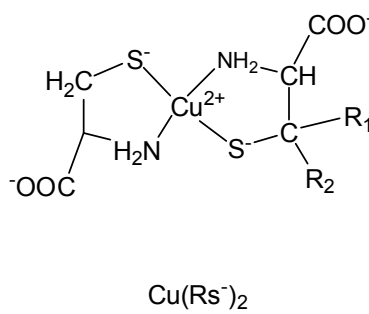
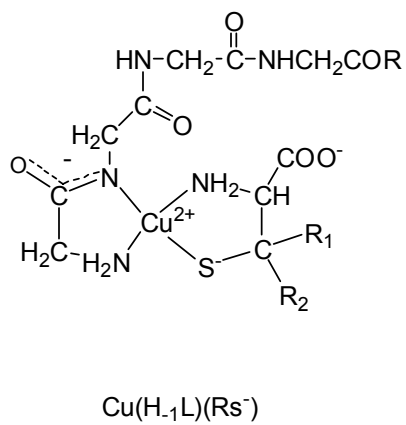
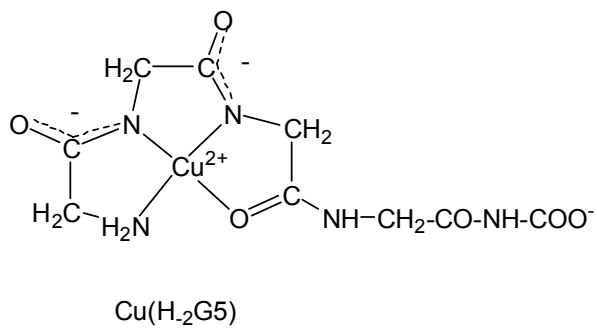
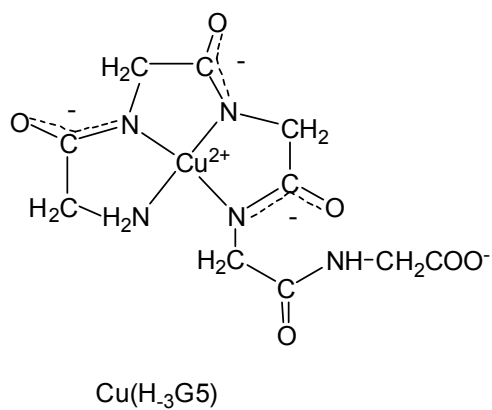
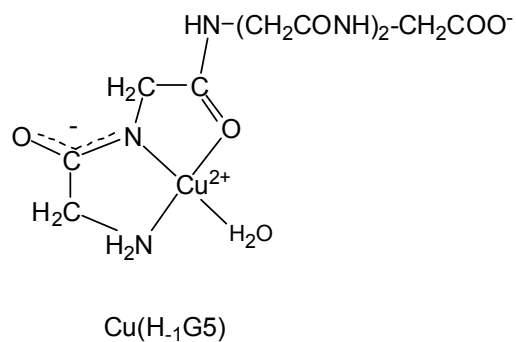
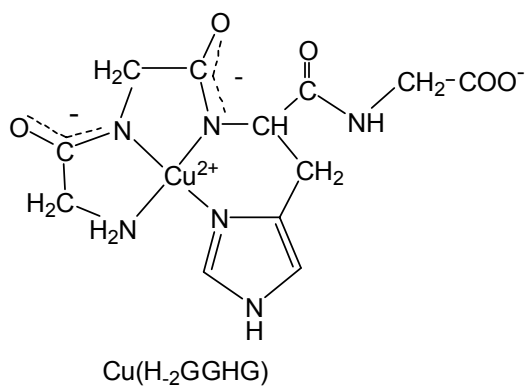


Fig. 1

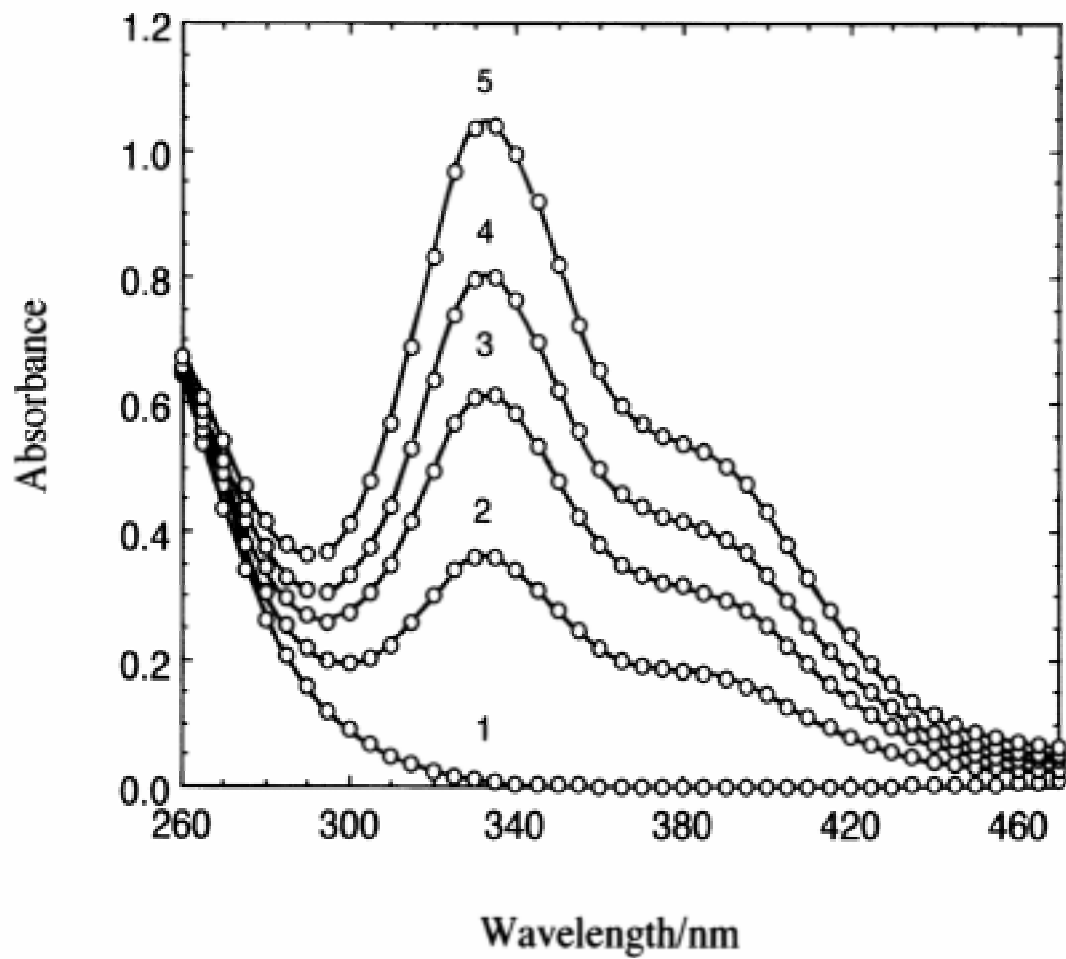


Fig. 2

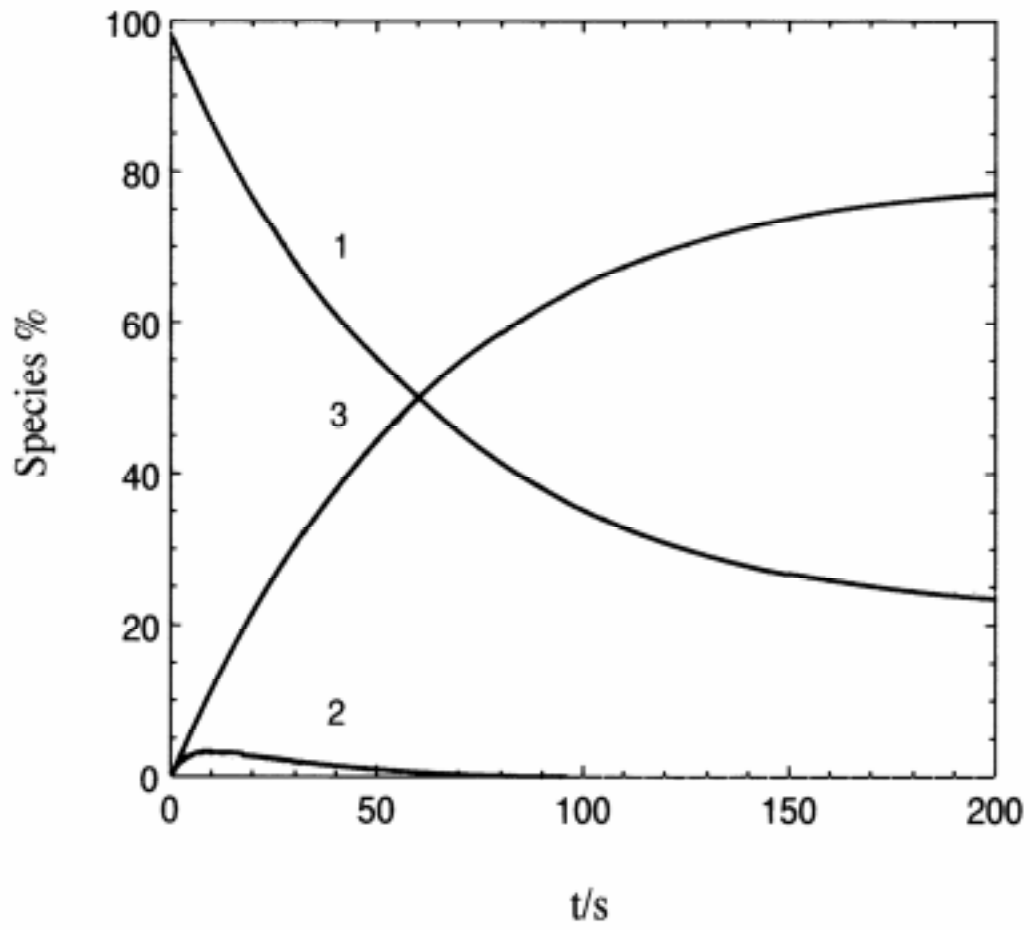


Fig.3

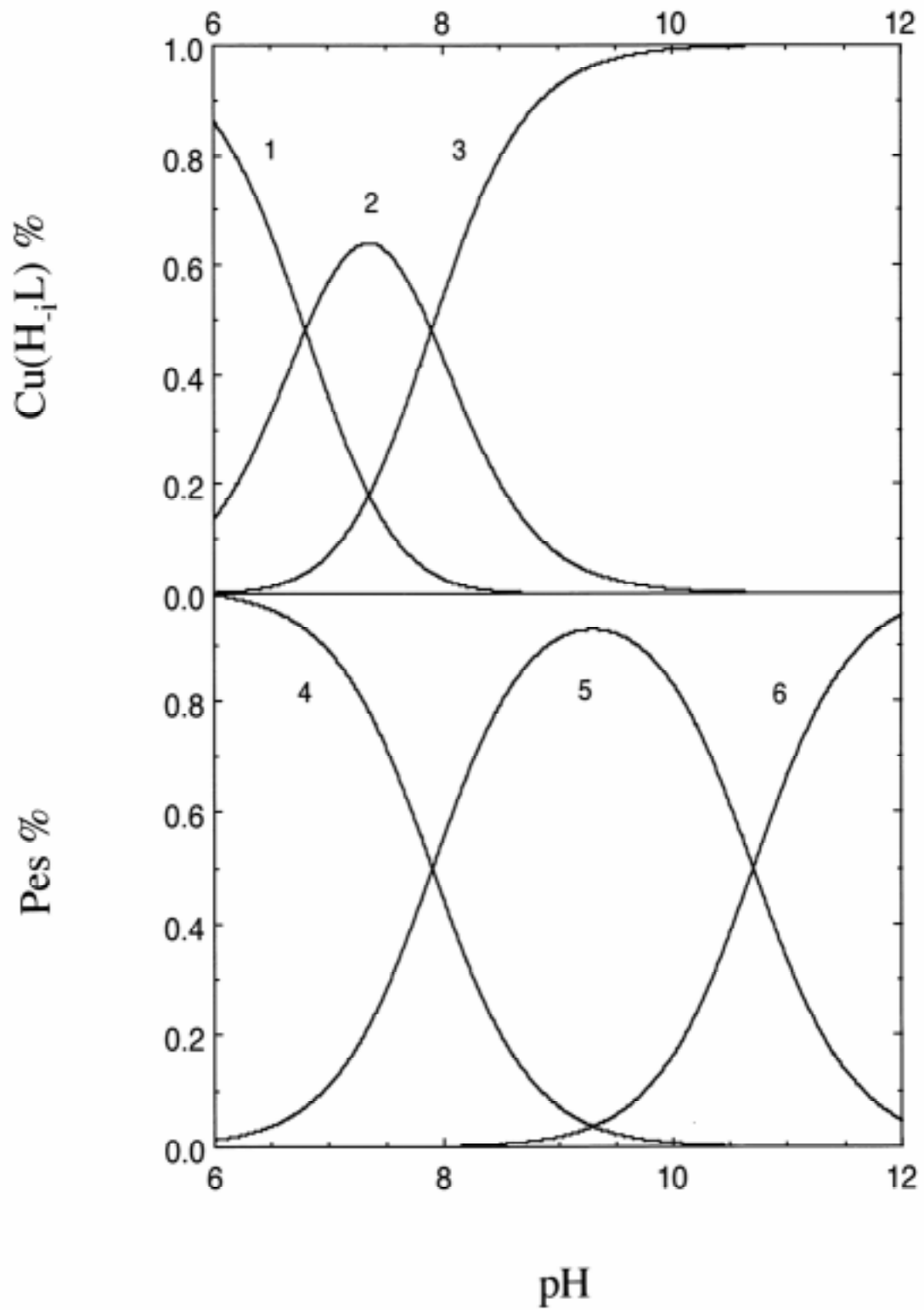


Fig. 4

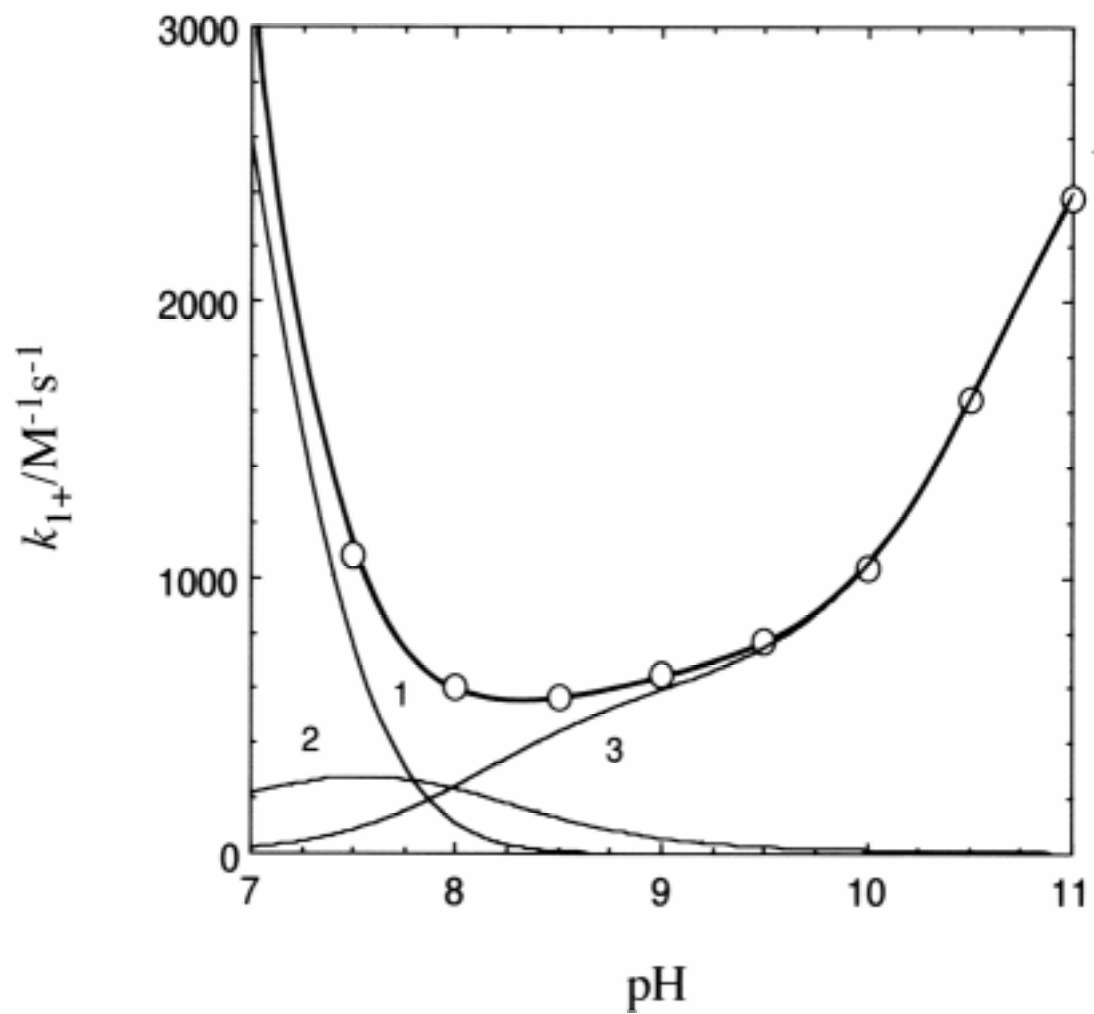


Fig. 5

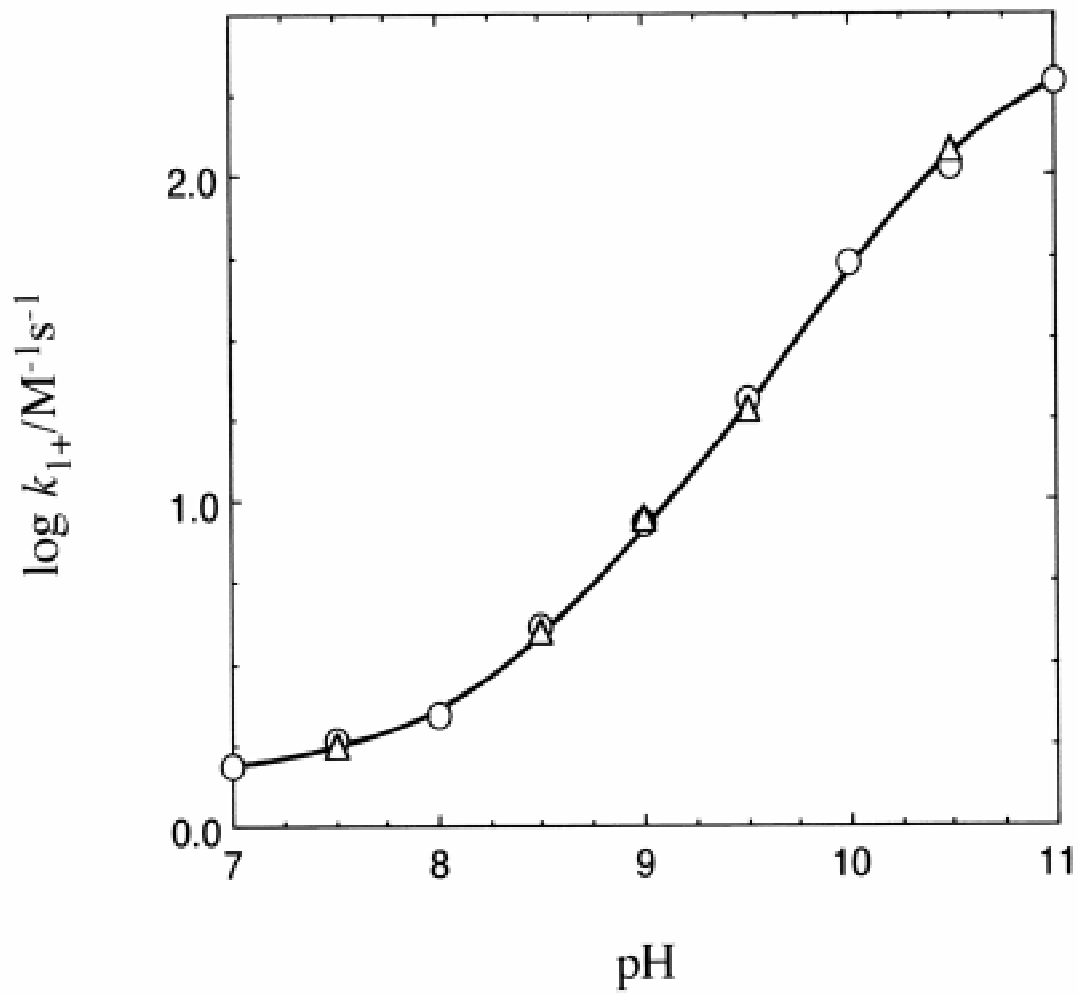


Fig.6

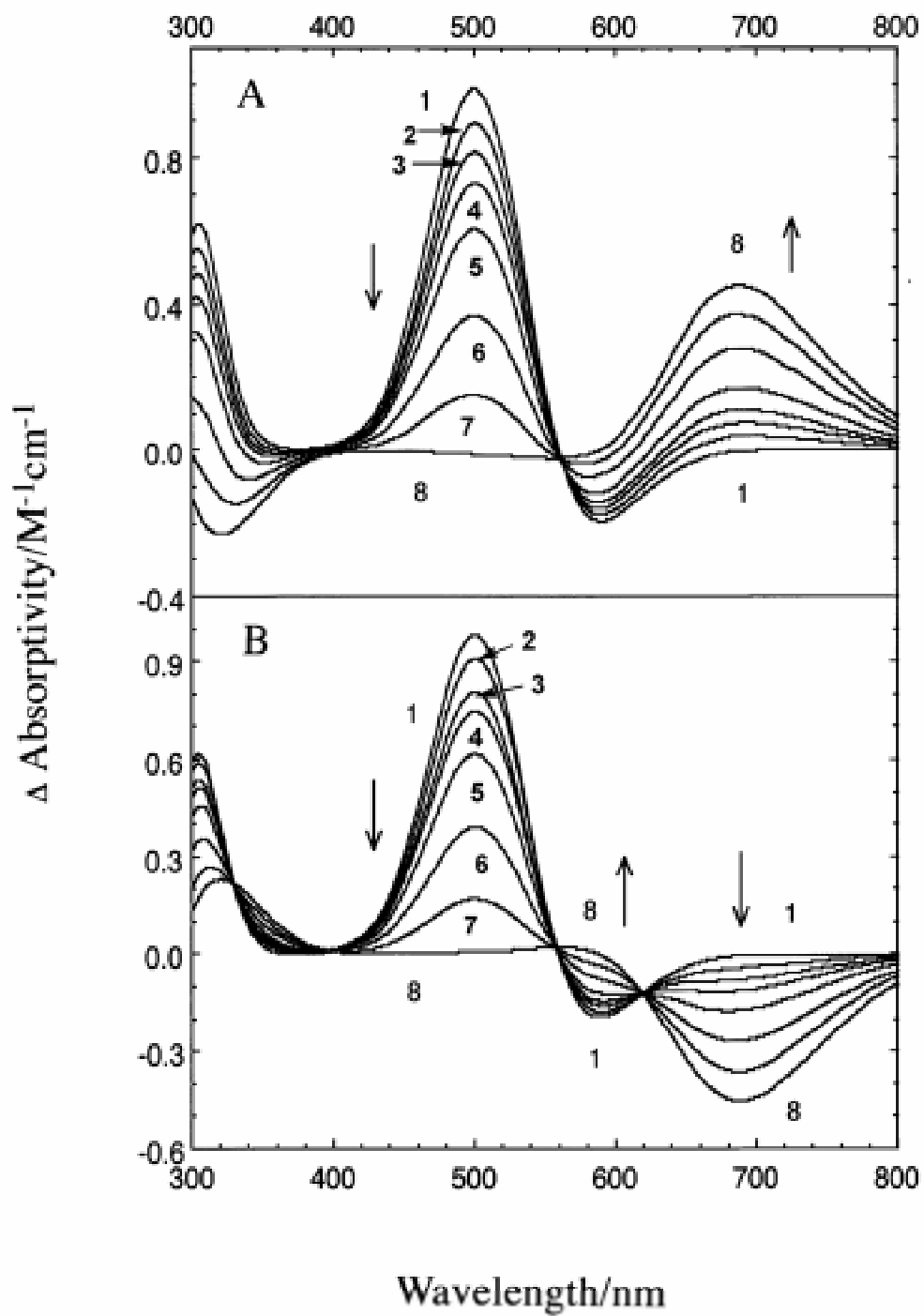


Fig. 7

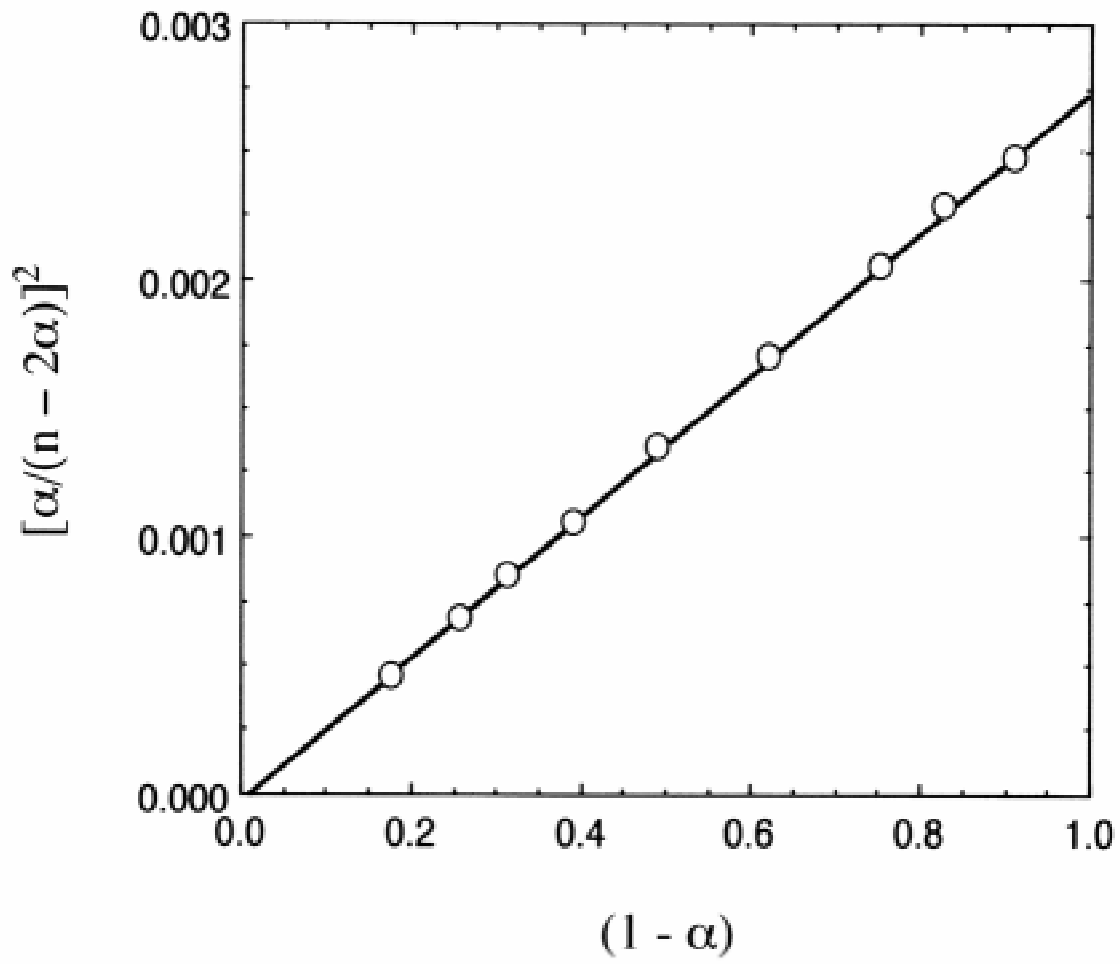
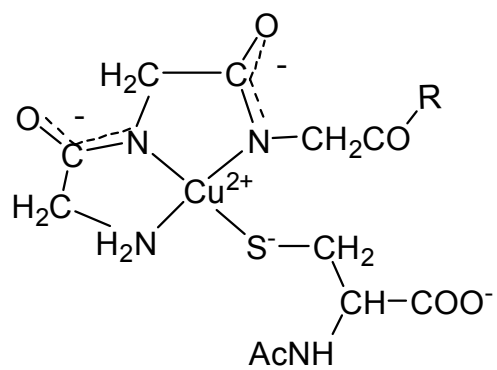
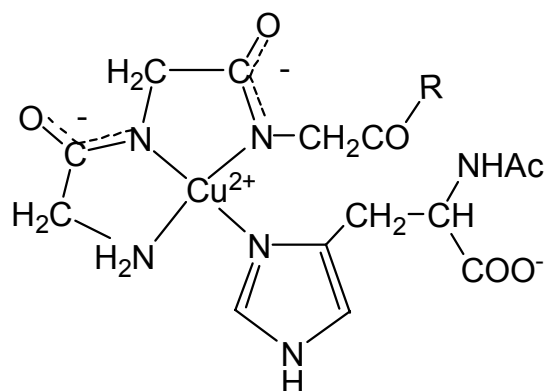


Fig. 8



Cu(H<sub>2</sub>L)(ACys<sup>-</sup>)



Cu(H<sub>2</sub>L)(ACHis)

Fig. 9

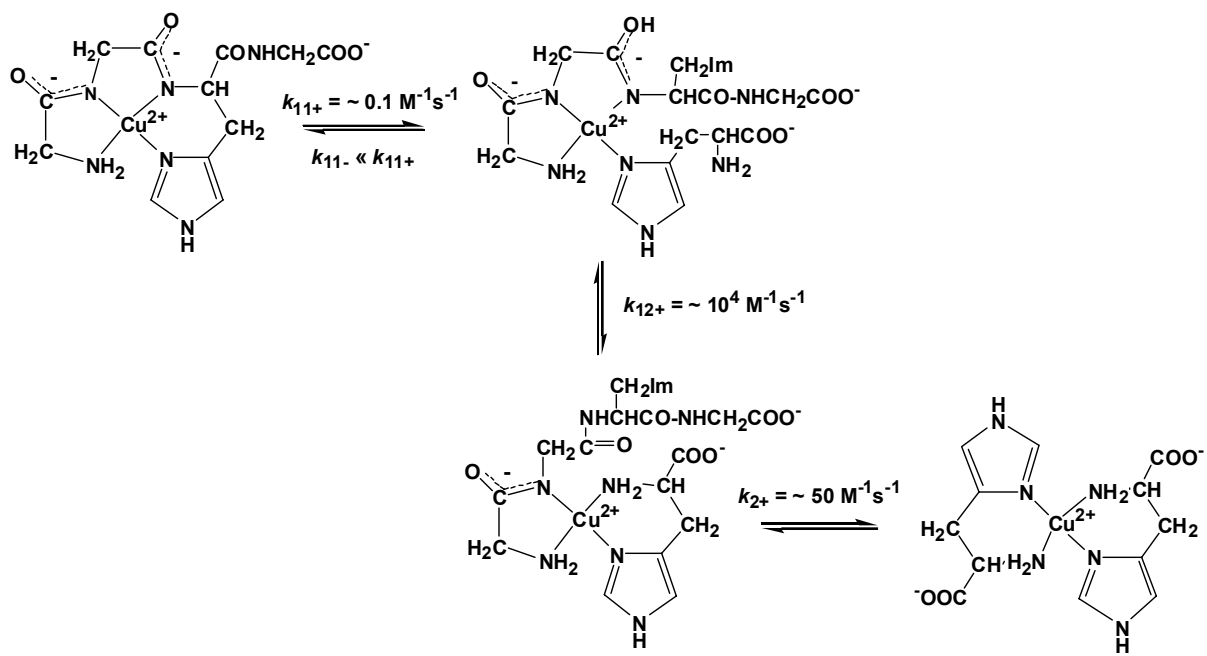
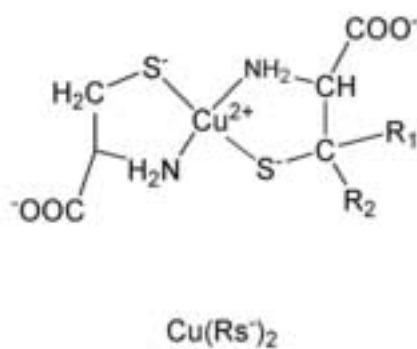
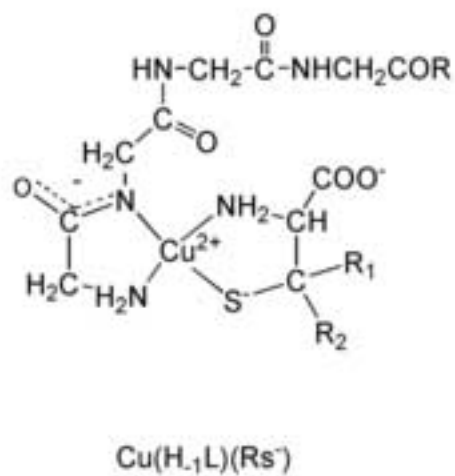
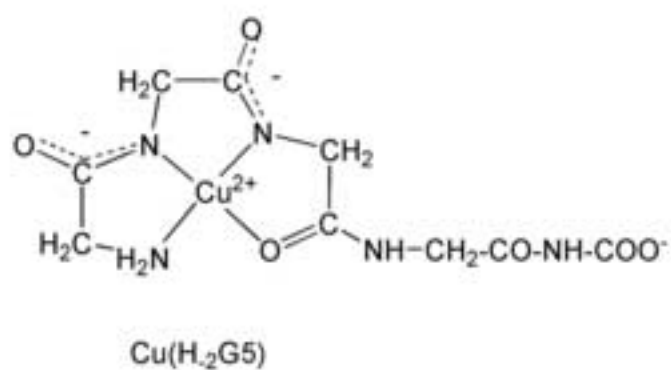
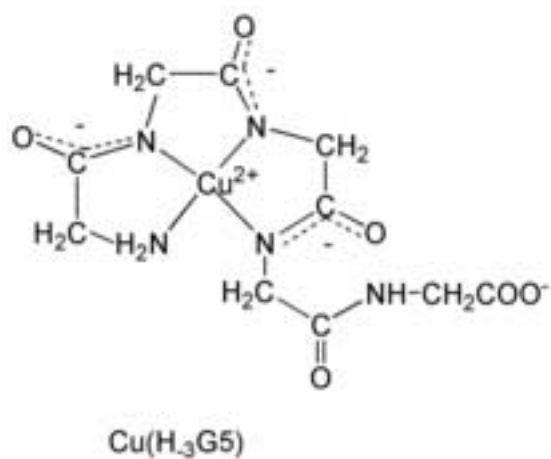
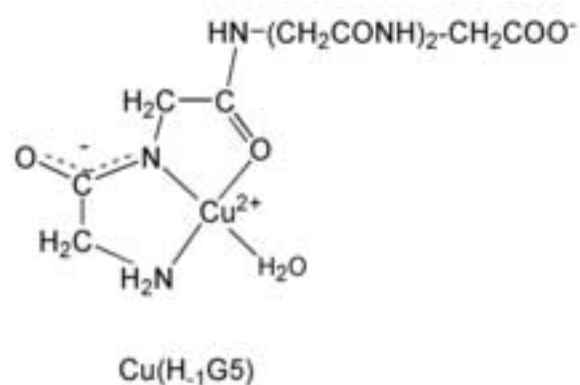
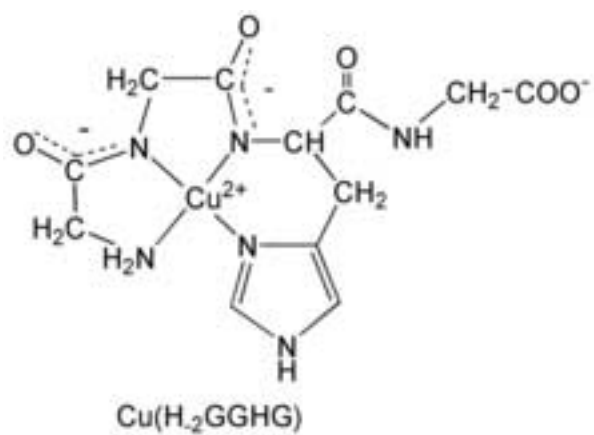


Fig. 10



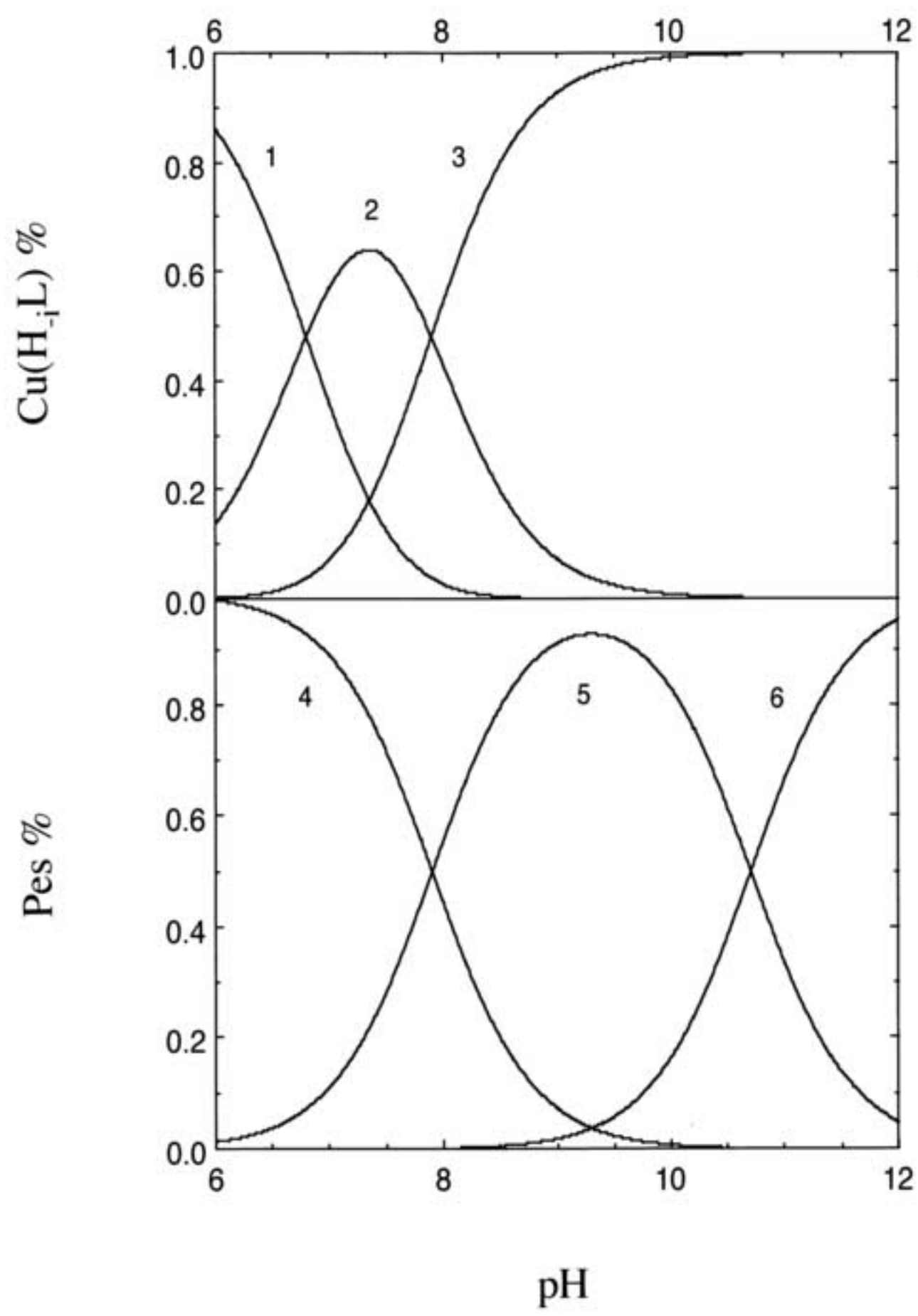
**Figure(s)**

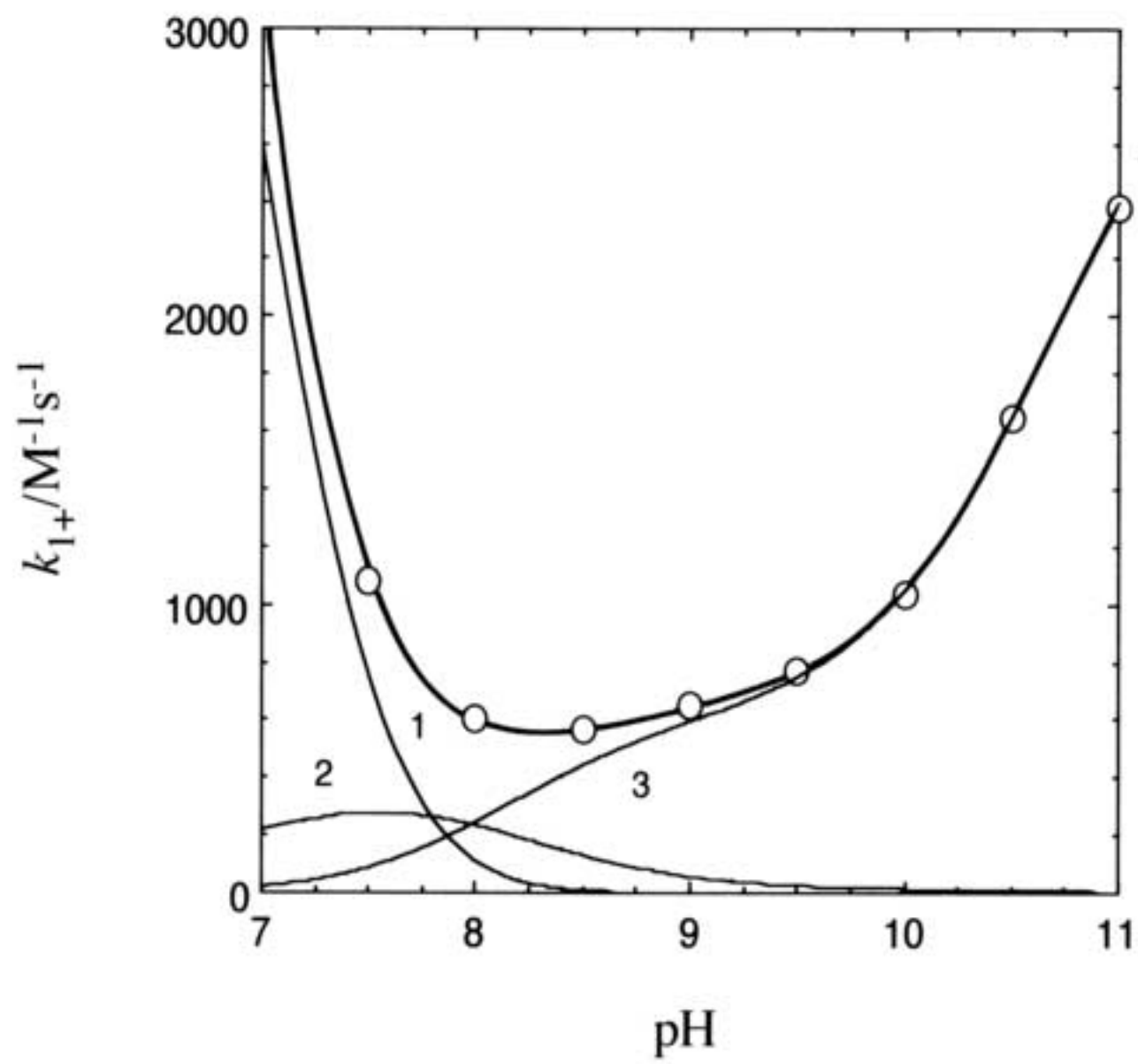
[Click here to download high resolution image](#)

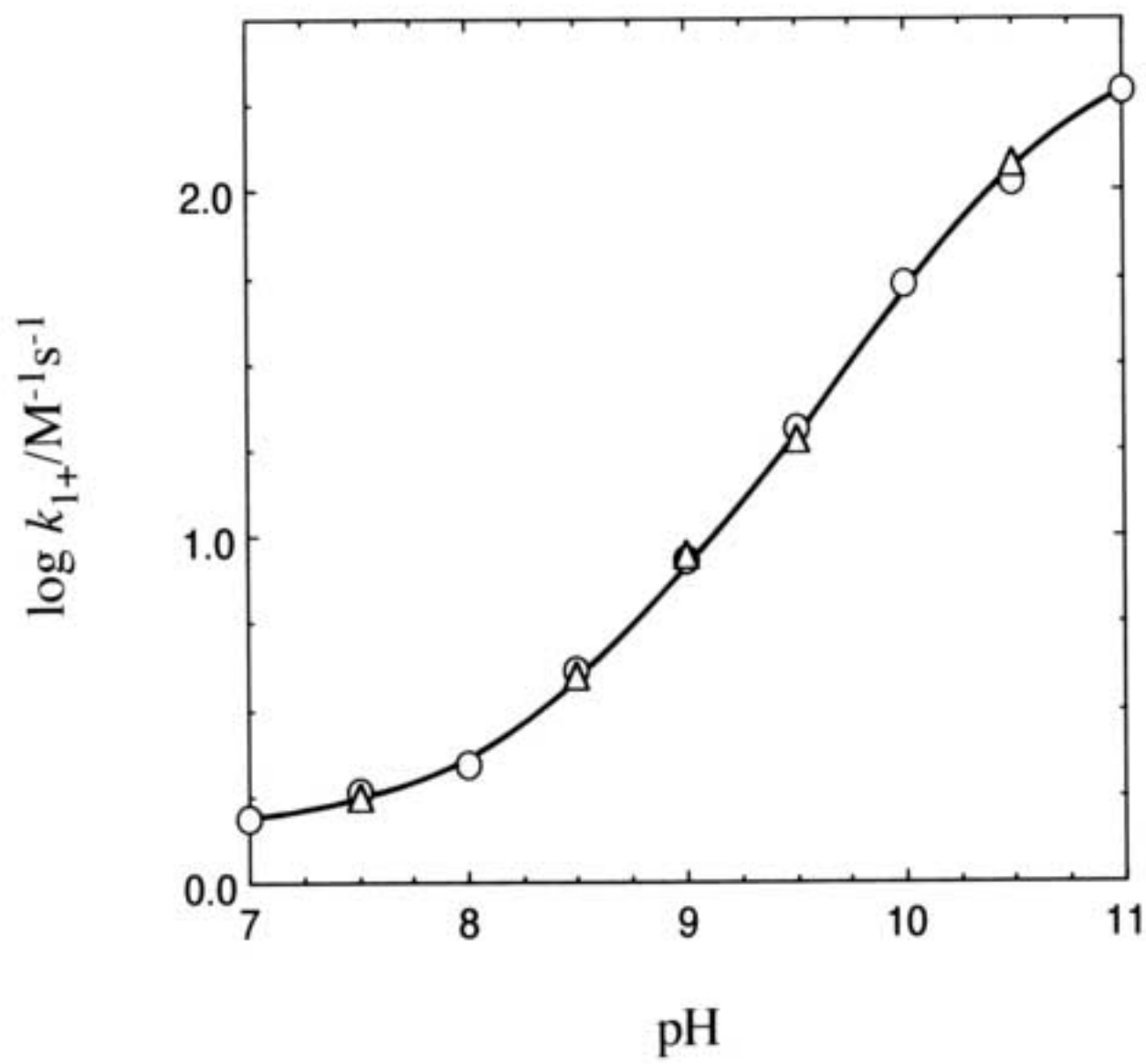
**Figure(s)**

[Click here to download high resolution image](#)

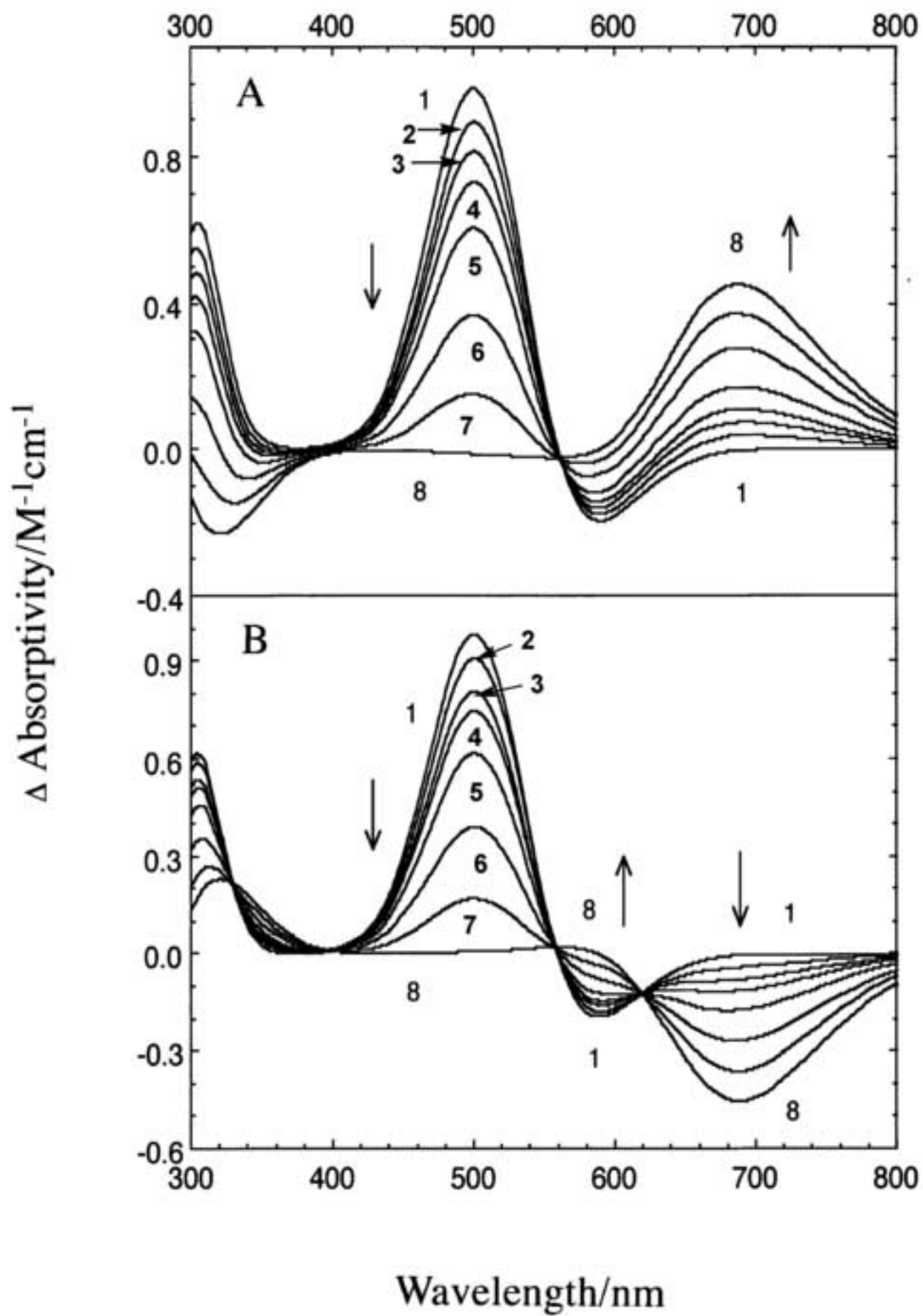
Figure(s)  
[Click here to download high resolution image](#)

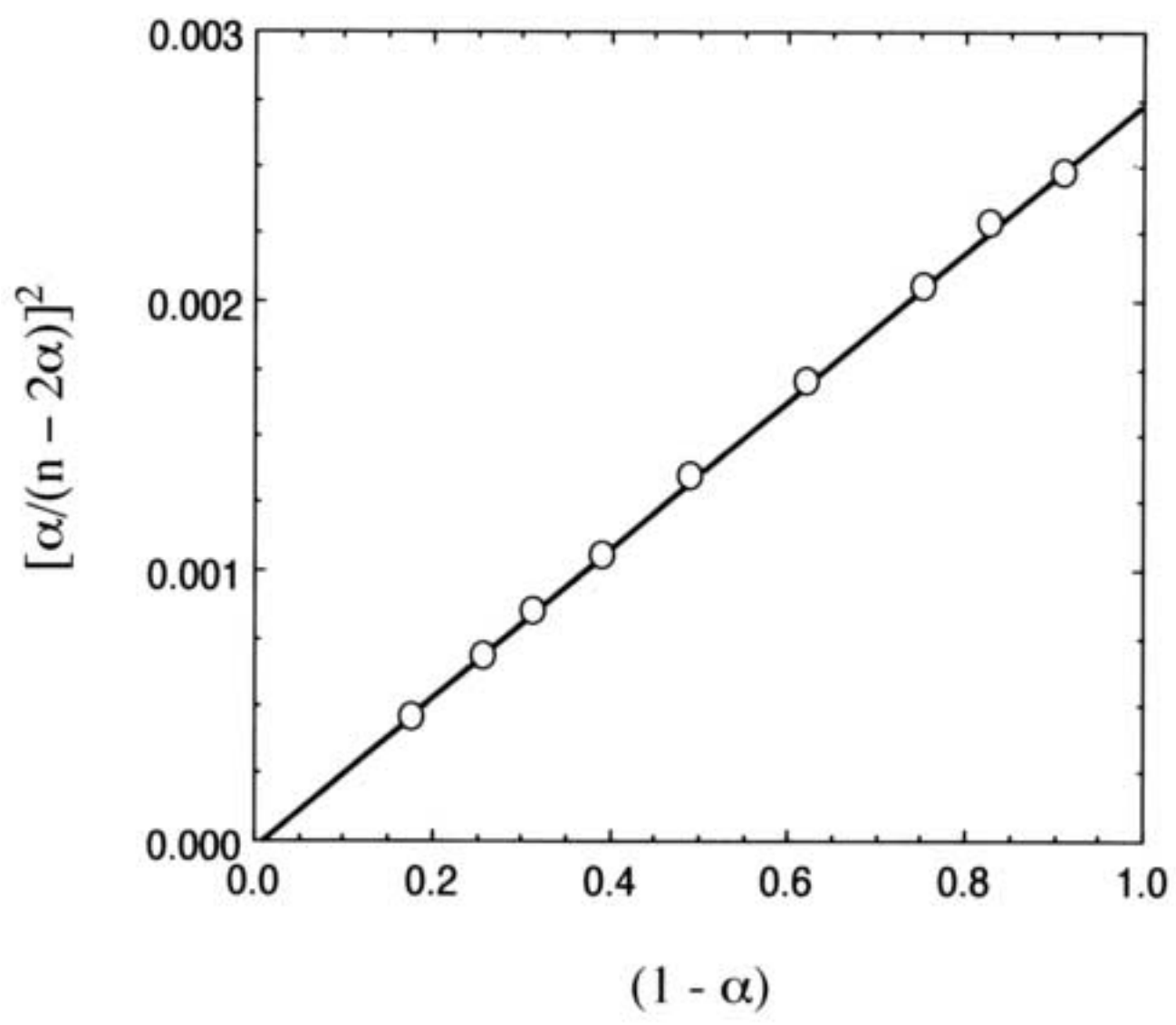






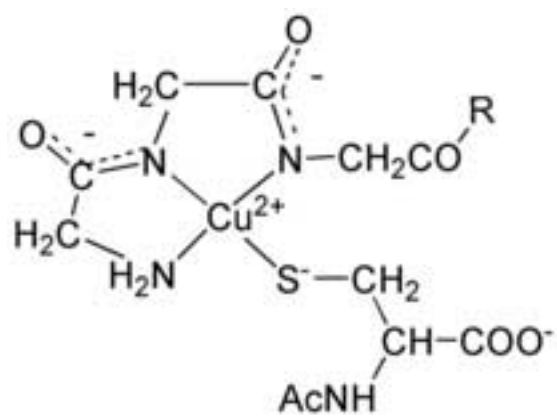
Figure(s)  
[Click here to download high resolution image](#)



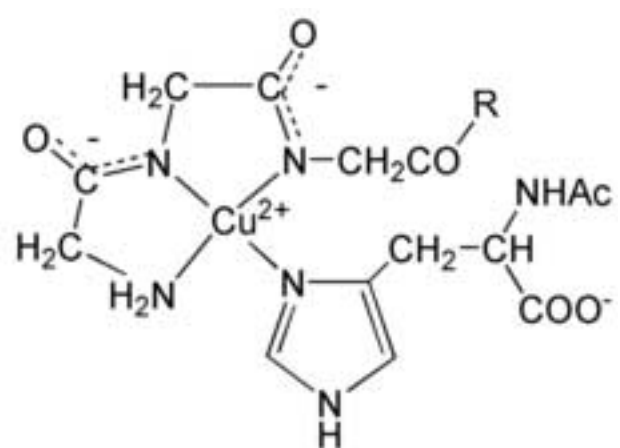


Figure(s)

[Click here to download high resolution image](#)



$\text{Cu}(\text{H}_2\text{L})(\text{ACys}^-)$



$\text{Cu}(\text{H}_2\text{L})(\text{ACHis})$

Figure(s)

[Click here to download high resolution image](#)